

**Title:** Complex Patterns of Local Adaptation in Teosinte

**Short title:** Local Adaptation in Teosinte

**Authors and affiliations:** Tanja Pyhäjärvi<sup>1</sup>, Matthew B. Hufford<sup>1</sup>, Sofiane Mezmouk<sup>1</sup> and Jeffrey Ross-Ibarra<sup>1,2,3</sup>

<sup>1</sup>Department of Plant Sciences, University of California, Davis, CA, USA.

<sup>2</sup>Center for Population Biology, University of California, Davis, CA, USA.

<sup>3</sup>The Genome Center, University of California, Davis, CA, USA.

**Corresponding author:** Jeffrey Ross-Ibarra

## Abstract

Populations of widely distributed species often encounter and adapt to specific environmental conditions. However, comprehensive characterization of the genetic basis of adaptation is demanding, requiring genome-wide genotype data, multiple sampled populations, and a good understanding of population structure. We have used environmental and high-density genotype data to describe the genetic basis of local adaptation in 21 populations of teosinte, the wild ancestor of maize. We found that altitude, dispersal events and admixture among subspecies formed a complex hierarchical genetic structure within teosinte. Patterns of linkage disequilibrium revealed four mega-base scale inversions that segregated among populations and had altitudinal clines. Based on patterns of differentiation and correlation with environmental variation, inversions and nongenic regions play an important role in local adaptation of teosinte. Further, we note that strongly differentiated individual populations can bias the identification of adaptive loci. The role of inversions in local adaptation has been predicted by theory and requires attention as genome-wide data become available for additional plant species. These results also suggest a

potentially important role for noncoding variation, especially in large plant genomes in which the gene space represents a fraction of the entire genome.

### **Author Summary**

Understanding how organisms adapt to different environments is a question of fundamental importance in evolution. Here, we investigated local adaptation in teosinte, the wild relative of domesticated maize. We find that the subspecies of teosinte studied here exhibit complex population structure, patterned by altitude, geography, dispersal events and admixture. We used dense genome-wide SNP genotyping to identify genetic variants likely associated with local adaptation. Our results point to a significant adaptive role for inversion polymorphisms, and reveal that the majority of variants differentiated among populations are found in noncoding regions of the genome. The size and complexity of most plant genomes suggests that our results may be indicative of an important role for structural and noncoding variants in the evolution of many plant species.

## Introduction

One of the enduring goals of evolutionary genetics is to understand the genomic and geographic extent of adaptation in natural populations. While many examples of adaptation in nature are known [1-4], our theoretical understanding [5-7] of the genomic signatures of adaptation has so far outpaced natural studies, and a number of outstanding questions remain. What are the prevailing forms (i.e. clinal, local) of adaptation in nature? What parts of the genome and what kinds of loci are involved? At what geographic scales can genome-wide signatures of adaptation be detected? The advent of high-throughput genotyping, however, is beginning to allow genomic analysis of populations across their natural range. For example, recent studies have shown geographically localized fitness effects [8], enrichment for nonsynonymous variants at adaptive loci [9] and adaptation across a number of environmental variables (e.g., soil type, temperature and precipitation) [8,10,11].

The wild relatives of domesticated maize offer an excellent opportunity to investigate these questions across a number of natural populations. In addition to the well-known domesticated maize, *Zea mays* ssp. *mays*, the species *Zea mays* includes three wild subspecies, collectively known as teosinte. Two of these, *Zea mays* ssp. *parviglumis* (hereafter *parviglumis*) and *Zea mays* ssp. *mexicana* (hereafter *mexicana*) are widespread taxa found in natural populations in central and southwest Mexico (Figure 1). Their combined range extends across varying environments, from the warmer low elevations of the Balsas River Valley to the cooler high elevations of Mexico's Central Plateau, across two-fold differences in precipitation and several soil types. Ecological niche modeling suggests that both

taxa have moved little in response to climate change during the Holocene (unpublished data), and their annual life history and outcrossing mating system have likely provided both the time and the genetic basis for adaptation to local conditions.

Previous work has investigated the genetic architecture of morphological differences in the teosintes [12-16]. Overall patterns of genetic diversity and structure in these taxa have also been detailed using various types of markers [17-20], but our understanding of genome-wide patterns of variation has been limited to a handful of accessions or comprehensive analyses of individual populations [21]. Even less is known regarding the genetics of local adaptation, which has only been studied at a few loci in the context of plant immunity [22].

Here we present a detailed population genetic examination of local adaptation across 21 populations of *mexicana* and *parviglumis* (Figure 1), based on high-density genotype data from 250 sampled individuals. We observed hierarchical population structure that correlated strongly with elevation. While patterns of haplotype sharing suggested relatively little gene flow between subspecies even in areas of sympatry, we nonetheless identified a highly admixed population at intermediate elevation. We then scanned the genome for potentially adaptive variants by looking for alleles associated with excess differentiation or correlation with environmental gradients. We identified several inversion polymorphisms and showed that these variants are enriched for signals of adaptation. Finally, we discuss the impacts of different selection pressures,

population structure, and geography on the ability to identify potentially adaptive variants using population genetic methods.

## Results

### Genomic diversity in teosinte

We sampled 21 populations of the wild subspecies *Zea mays* ssp. *parviglumis* and *Zea mays* ssp. *mexicana* from across their native ranges in central and southern Mexico (Figure 1). Ten to twelve individuals from each population were genotyped using the Illumina MaizeSNP50 chip. After quality control, the full dataset consisted of 248 samples genotyped at 36,719 SNPs.

Both *parviglumis* and *mexicana* showed generally high levels of heterozygosity and little evidence of inbreeding, and the relatively minor differences in the overall distribution of heterozygosity between the subspecies suggest a relatively limited impact of SNP ascertainment on comparisons of diversity (Figure S1). Considerable variation was evident among populations in both taxa, however (Figure 2, Table S1). The *parviglumis* population of Los Guajes, for example, showed the signs expected of a large outcrossing population, including high diversity, an inbreeding coefficient ( $F_{IS}$ ) close to zero, no deviation from Hardy-Weinberg equilibrium, and relatively brief runs of homozygosity (ROH, Figure S2) across the genome. Other populations, however, showed evidence of past demographic change: diversity in San Lorenzo *parviglumis* was only half that of Los Guajes, and *mexicana* individuals from Xochimilco were characterized by extremely long ROH and extensive within-population haplotype sharing, consistent with a recent population bottleneck.

Patterns of linkage disequilibrium (LD) varied greatly along the genome, with numerous discrete blocks of elevated LD observed in multiple populations. We identified four large (>10Mb) regions of high LD ( $r^2 \geq 0.2$ ), which we interpreted here as inversion polymorphisms (Figure 3, Figure S3). Three of these regions appeared to correspond to inversions previously described cytologically (*Inv9e*; [23]), in mapping populations (*Inv4m*, [24]), or by population genetic analysis (*Inv1n*, [25,26]). Clear haplotype structure was observed for three of the putative inversions, and simple genetic distance-based clustering including *Tripsacum* and maize suggested that the non-maize haplotype was likely the derived state (Figures S4-S7).

### Population structure

Signs of population structure in teosinte were evident at multiple hierarchical levels. The strongest signal was between subspecies, shown in the principle component analysis (PCA), where the first PC separated the two subspecies and explained ~11.5 % of the total variance (Figure 4A). Differentiation between subspecies was also evident in STRUCTURE results (Figure 4B), haplotype sharing (Figures S8-S9), and in higher pairwise  $F_{ST}$  for inter-subspecific (0.33) than intra-subspecific (*parviglumis* 0.24; *mexicana* 0.23) comparisons. Inversion polymorphisms also separated the subspecies, as *Inv9d* and *Inv9e* were found only in *mexicana*, while the derived haplotypes at *Inv1n* and *Inv4m* showed strong frequency differences (Figure S10) among subspecies.

Additional levels of structure were observed within subspecies as well (Figure S11). STRUCTURE and PCA analysis of populations of *parviglumis* identified

groups of related populations consistent with previous groupings [17]. Although substructure within *parviglumis* identified a grouping of populations in Jalisco known to be near cultivated maize, [16], a joint STRUCTURE analysis including a diverse sampling of 279 maize inbred lines [27] failed to find evidence that admixture explains the observed population structure (Figure S12). In all, 20 significant principle components identified 21 clusters that generally corresponded to sampling locales (Figure 4A, Figure S13). Three populations of *parviglumis* did not follow this trend, however, as the two Ejutla populations formed a single genetic cluster and the Ahuacatitlan population split into two clusters.

Both geodetic distance (Mantel test p-value: 0.006, Mantel statistic  $r = 0.40$ ) and altitude (p-value: 0.0008,  $r = 0.37$ ) appeared to correlate with population differentiation in the combined dataset (Figure S14A; partial Mantel tests for geodetic distance p-value: 0.0005,  $r = 0.39$ ; altitude p-value: 0.004,  $r = 0.41$ ). Although the proportion of *mexicana* ancestry appeared to increase with altitude in STRUCTURE results (Figure 4B), differentiation within each subspecies was only significantly correlated with geodetic distance (p-value: 0.004,  $r = 0.55$  in *parviglumis*; p-value: 0.046,  $r = 0.48$  in *mexicana*; Figure S14 B and C). In both subspecies the correlation with geodetic distance appeared to be primarily due to the peripheral Nabogame and Oaxaca populations and was no longer significant when these were removed from the analysis.

Finally, both STRUCTURE and PCA results suggested that the Ahuacatitlan population of *parviglumis* may be admixed (Figure 4). Consistent with this, analysis of haplotype sharing showed that the Ahuacatitlan population shared fewer long

haplotypes with *parviglumis* and more long haplotypes with *mexicana* than any other *parviglumis* population (Figure S8 and S9). The average length of shared haplotypes between Ahuacatitlan and *mexicana* (mean 4.8 cM), however, was shorter than the average length of haplotypes shared among *mexicana* populations (mean 30.7 cM), arguing against extensive recent admixture. To explicitly test the position of Ahuacatitlan with respect to the two subspecies, we applied the D-test of derived allele configuration devised by Green et al. [28]. The observed distribution of D was inconsistent with models in which Ahuacatitlan is ancestral to both *parviglumis* and *mexicana* or a sister group to *mexicana* ( $p < 0.05$  for both; Figure S15), while the model in which Ahuacatitlan was sister to *parviglumis* could not be rejected ( $p < 0.2$ ).

#### Candidate SNP identification

We applied three approaches to identify SNPs underlying local adaptation, and candidate SNPs and genes from each of these approaches are listed in Table S2. We first applied the environmental association method implemented in BAYENV [29] to a set of 76 climate and soil variables. We summarized these variables with 6 principle components which represent 95% of the variation among populations. We calculated environmental PCs and estimated Bayes factors for the joint data set and for each subspecies separately (Table 1, Figure S16-S18), and retained SNPs consistently in the top 5% of Bayes factors and in the top 1% of average Bayes factors across 5 runs of the BAYENV MCMC. In the joint data set, in total 1598 SNPs were associated with at least one PC, while 54 SNPs were associated with more than one PC. The number of candidates was lower within subspecies, where 370 SNPs in



*parviglumis* and 533 SNPs in *mexicana* were associated with at least one of the four PCs representing 95% of within subspecies environmental variation.

Our second approach to identify locally adapted SNPs used an  $F_{ST}$  outlier method [7,30] to scan for SNPs showing an excess of differentiation between subspecies ( $F_{CT}$ ) or among populations ( $F_{ST}$ ). Hierarchical analysis yielded 731  $F_{CT}$  (2.0%) and 1363  $F_{ST}$  (3.7%) outliers in the 1% tail of simulated values. A striking peak in differentiation was observed within inversion *Inv4m*, which showed 12-fold and 6-fold enrichment of outlier SNPs for  $F_{CT}$  and  $F_{ST}$ , respectively. Both sets of outliers (Figure 5A, Figure S19, Table S2) differed substantially compared to SNPs identified by BAYENV (Table S3). The strongest correlation (Spearman's rho -0.20,  $p \ll 0.001$ ) was seen with Bayes factors for PC2 in the joint data set and p-values of  $F_{ST}$  (Figure 5A).

Finally, we performed a scan for SNPs highly differentiated in a single focal population, which we called an  $F_{FT}$  outlier approach (see Materials and Methods). Mean  $F_{FT}$  across populations was lower than 0.1, suggesting that genome-wide only a small proportion of the total genetic structure was due to drift in individual populations. The 1% tails (354-358 SNPs in each population) of the  $F_{FT}$  distribution did not overlap considerably with  $F_{ST}$  (Figure 5B) and Spearman's correlation coefficient was not significant for any of the  $F_{FT}$  in relation to  $F_{ST}$  or  $F_{CT}$  values. Populations at range extremes, such as El Rodeo and Nabogame, tended to have higher  $F_{FT}$  (1% cutoff at 0.79 and 0.72), and high  $F_{FT}$  SNPs from these populations were also overrepresented among  $F_{ST}$  (Figure S20; Wilcoxon rank sum test  $p$ -values  $\ll 0.001$ ) and BAYENV outliers. The most striking case was the effect of the

Nabogame population on association results for PC2 (Figure S21), where SNPs with high  $F_{FT}$  in Nabogame had significantly higher Bayes factors than  $F_{FT}$  outliers of other populations (Wilcoxon rank sum test p-value  $\ll 0.001$ ). Nabogame  $F_{FT}$  outliers constituted  $\sim 9\%$  of all PC2 outliers for BAYENV, and PC2 Bayes factors were positively correlated with  $F_{FT}$  in Nabogame (Spearman's rank correlation p-value  $\ll 0.001$ ,  $\rho=0.21$ ).

All four inversions contained an excess of SNPs with high  $F_{ST}$  or were enriched for SNPs associated with environmental variables (Figure 6, Table 2). Inversions were 2-fold enriched for candidate SNPs (p-value  $< 0.0001$ ), containing 5.6% of all SNPs but 11 % of SNPs in the 99th percentile of the maximum rank distribution of our candidate lists. Enrichment was most notable for PC1, which predominantly reflected variation in altitude and annual temperature. As reported in Fang et al. [26], the inverted arrangement of *Inv1n* showed an altitudinal cline, occurring at intermediate frequency in most *parviglumis* populations and at low frequency in *mexicana* (Figure S4 and S10A). The trend was less clear in our data, however, as the derived arrangement of *Inv1n* was absent from the low elevation Crucero Lagunitas population of *parviglumis*. Two additional inversions showed similar altitudinal patterns: the derived arrangement in *Inv4m* was most abundant in high elevation *mexicana* populations and restricted to the highest elevation *parviglumis* population, (Ahuacatitlan; Figure S10B), whereas the non-maize arrangement of *Inv9d* was found only in the highest elevation *mexicana* populations (Figure S10C, Figure S22A).

### Functional evaluation of candidate SNPs

We tested candidate SNPs for enrichment in various functional categories (genic vs. non-genic, synonymous vs. nonsynonymous) as well as for associations with maize phenotypic traits [31,32] and regions highlighted as putative adaptive introgressions from *mexicana* into maize (unpublished data). Among genes that showed evidence of introgression from *mexicana* into maize both  $F_{ST}$  (p-value <0.0001) and  $F_{CT}$  (p-value 0.0002) candidates as well as SNPs associated with PC2 within *mexicana* (p-value 0.0061) were more common than expected by chance.  $F_{ST}$  outliers were strongly enriched for non-genic SNPs (permutation p-values = 0.001) (Table S4), a result that held even after excluding SNPs in the four identified inversions (data not shown).  $F_{ST}$  outliers were also enriched for SNPs associated with male inflorescence architecture and stand count (plant survival and density) in a maize panel (Table S5). Finally, SNPs associated with flowering time were not over-represented under an association model that takes into account structure (both  $K + Q$ ; see Materials and Methods), but were significantly over-represented among both  $F_{CT}$  and  $F_{ST}$  outliers when correction for population structure was not applied (Table S6). The collinearity between the structure and flowering time adaptation makes it difficult to control the structure without increasing the rate of false negatives, whereas without a control of the structure all true positives are kept but the rate of false positives is high. The latter is conservative when testing for an enrichment for the adaptive loci.

The functional annotations of nearby or containing genes were investigated for six SNPs that were extreme outliers for  $F_{ST}$  (Figure S19). Of these, PZE-104028461 is a synonymous SNP in the maize filtered gene GRMZM2G000471,

whose ortholog AT4G10380, *NIP5;1*, encodes a boron channel [33]. The high  $F_{ST}$  in this gene is caused by an allele fixed in the Nabogame population that is found only in two heterozygotes in the rest of the sample. The SNP is also significantly correlated with PC2 within *mexicana*. In *Arabidopsis thaliana*, SNPs associated with *in planta* boron concentration were enriched among SNPs showing strong signals of selection [34], and AT4G10380 was also identified as a candidate gene for adaptation to different soil types in *Arabidopsis lyrata* [35].

## Discussion

### Complex population structure

Our results indicate that population structure in teosinte is complex and affected by multiple factors. Across all populations, the effects of altitude on population structure are significant, even after correcting for geodetic distance (Figure S14A). The *mexicana* populations of Santa Clara and Opopeo, for example, show higher  $F_{ST}$  with the La Cadena *parviglumis* population 60 km away than with distant *parviglumis* populations at the same elevation (Figure S23). These results are in agreement with earlier studies that have noted the important role of altitude on genetic distance, genome size and morphological characters in *Z. mays* subspecies [36-39]. There is also clear hierarchical population structure (Figure 4, Figure S11), with divisions between subspecies and among previously identified groupings within subspecies [17]. Within subspecies, the effect of altitude is no longer statistically significant, but isolation by distance continues to explain a meaningful portion of the genetic structure observed in both taxa (Figure S14B and S14C). In addition to distance and altitude, stochastic founding events have likely played a

role in patterning diversity. This is most evident in the extensive haplotype sharing within the geographically dispersed La Mesa/El Sauz/San Lorenzo group (Figure S8). The importance of founder events is consistent with previous analyses by Fukunaga et al. [17] and Buckler et al. [37] who found that genetic distance was more correlated with specific dispersal routes than with geodetic distance.

While hybridization between *mexicana*, *parviglumis* and cultivated maize is a well-known phenomenon [17], the extent of admixture between the two wild subspecies has not been well documented. Our data suggest that the high elevation *parviglumis* population is extensively admixed, with mean assignment probabilities to *mexicana* ~50% for all individuals in the population. Patterns of haplotype sharing (Figure S8-S9) and derived allele counts (Figure S15), however, support a model of continual gene flow with *parviglumis* over a relatively long period of time. Ross-Ibarra et al. [40] proposed a demographic model including continuous gene flow between *mexicana* and *parviglumis* apparently inconsistent with the general lack of admixture and strong differentiation we observe here for most populations. We note, however, that several of the *parviglumis* individuals sampled by Ross-Ibarra et al. are from localities quite near Ahuacatitlan, including two collected only ~4 km away. Fukunaga et al. [17] also identified a number of putative *mexicana* – *parviglumis* hybrids from localities in the Eastern Balsas near to Ahuacatitlan. Together with our results showing no admixture in *parviglumis* populations such as La Cadena and Los Guajes that are in geographic proximity to *mexicana*, these data indicate the presence of a geographically restricted hybrid zone between *mexicana* and *parviglumis* occurring at mid elevations in the Eastern Balsas region.

Population structure can bias estimates of demographic history and the inference of selection through its effect on the allele frequency spectrum [41]. In addition, Eckert et al. [11] point out that when environmental and population structure gradients coincide, environmental correlation methods may suffer from over-correction of structure. To resolve biased demographic inference caused by sampling, several authors have shown that sampling single individuals from each of many populations largely ameliorates this bias under simple island [42] or stepping stone [43] models. However, such a sampling scheme does not take into account uneven or hierarchical population structure, [44]. In teosinte, hierarchical population structure is observed within individual subspecies and is patterned by both geography and the environment. We have also shown that populations at the edge of the range, like Nabogame and El Rodeo, are unusually distinctive. Because most plants likely show complex patterns of structure, it is clear that careful population level sampling and consideration of population structure is important in studies of plant adaptation and evolutionary history.

### **The genetic basis of local adaptation in teosinte**

In contrast to the results of similar analyses in *A. thaliana* and human data [9,45], enrichment of neither genic nor nonsynonymous sites was observed among candidate SNPs (Table S4). While the SNP chip developed for maize is less dense than the human or *Arabidopsis* data, it nonetheless samples the gene space of maize quite well, suggesting that SNP density or the makeup of the chip does not explain the difference in nonsynonymous sites. And though the positive correlation between Bayes factors and heterozygosity may lead to biases among SNP categories,

the average expected heterozygosity of nongenic SNPs in our data was slightly lower than for genic SNPs (0.275 vs. 0.281). Instead, it seems likely that the complexity of the maize genome, which is more than 85% noncoding sequence [46], may provide greater opportunity for the evolution of functional noncoding elements. The causal quantitative trait loci (QTL) for several well-studied genes has been shown to reside in noncoding regions near genes [e.g., 47,48], and noncoding SNPs have recently been shown to explain the majority of associations for morphological traits [49]. The functional role of candidate SNPs is supported by their enrichment among relevant phenotypic effects (Table S5 and S6). SNPs associated with tassel morphology, that is a major phenotypic difference among *parviglumis* and *mexicana* [50], are enriched among  $F_{CT}$  candidates. Further, SNPs associated with flowering time—a common adaptation among plant populations [e.g., 51,52]—are also highly differentiated among populations and subspecies.

In spite of the lack of genic enrichment, we do identify a number of likely candidate genes for local adaptation (Table S2). A SNP in the gene *b1*, for example, was found correlated with PC1—which is largely made up of temperature and altitude—among *mexicana* populations. *b1* is a gene in the anthocyanin synthesis pathway that has been identified as a QTL for sheath color differences among *mexicana* and *parviglumis* by Lauter et al. [12], and pigmentation has been suggested to be an important plant adaptive trait as a response to lower temperatures and changing light conditions [53,54]. Two SNPs in the 3'UTR of the well-known domestication gene *tb1* show unusually strong patterns of differentiation and association with PCs related to temperature range and soil types

(Table S2). *tb1* is a transcription factor that had a significant role in morphological changes during maize domestication [47,55], and SNPs in the 3' UTR have previously been found to be significantly associated with lateral length and tassel branching in *parviglumis* [14,15]. Other candidate genes that have a well known function in maize are, for example, *abph1* [56] and *sh1* [57].

In addition to the rich nucleotide diversity of teosinte, cytological studies of both *mexicana* and *parviglumis* have identified a number of inversion polymorphisms [13,23,58]. In our high density genotyping data we observe four blocks of LD that we interpret as putative inversions. *Inv1n* was described by Fang et al. [26]. *Inv9e* was identified cytologically by Ting [23], who found the inverted arrangement at high frequency in both of the *mexicana* populations in which we see the derived haplotype. Similarly, the LD block we identify as *Inv4m* is in a similar physical position as inversions identified cytologically in maize and teosinte [13,23], and by marker map order in the progeny of a self-fertilized *Zea nicaraguensis* [24]. Synteny maps identify the proximal breakpoint of *Inv4m* as the junction of a chromosomal fusion with the distal end of the telomere of chromosome 5 [Figure S15 in 46], and the breakpoint is common to several distinct inversions in maize [59], suggesting that the region may be prone to structural rearrangements.

All four observed inversions appear to play a role in local adaptation. All show significant enrichment for SNPs with high Bayes factors for PC1 (Table 2), reflecting environmental differences in altitude and temperature. Inversion *Inv1n* is enriched for SNPs with high Bayes factors for PC1, PC3 and PC4, and the clinal patterns observed are consistent with those of Fang et al. [26] with the exception of



the Crucero Lagunitas population which was not polymorphic for the inverted allele. Extreme patterns of precipitation in Crucero Lagunitas and shared ancestry with the distant Oaxacan population of El Rodeo suggest that unusual history or distinct selection pressures may help explain the surprising lack of *Inv1n* in this population. *Inv4m* is associated with a striking peak in differentiation among subspecies (Figure 5). This is consistent with an adaptive role for *Inv4m* at higher altitudes, which was also suggested by the evidence of introgression from *mexicana* to sympatric maize populations at *Inv4m* and its rarity in maize outside of the Mexican highlands (unpublished data). Interestingly, QTL for differences between *parviglumis* and *mexicana* for pigment intensity and macrohair count, traits thought to be adaptive at high elevations, co-localize to this region as well [12]. *Inv9d* was only polymorphic in *mexicana* and showed a strong enrichment of SNPs associated with PC1 (Figure 5, Figure S22B). Finally, though not strongly associated with altitude, inversion *Inv9e* showed 8-fold enrichment of SNPs associating with PC4 (top soil) within *mexicana* (Table 1, Figure S18D).

Our evidence suggests that all four inversions carry important adaptive variation, but further experiments such as association mapping and reciprocal transplant experiments will be required to directly measure their effects on phenotype and fitness. The accumulation of locally adaptive loci in inversions has long been predicted by theory [60], and is consistent with observations in a number of plant and animal taxa [61-65]. One of the major effects of chromosomal inversions is to suppress recombination, because inversions that capture two or more locally beneficial alleles may be favored by selection [60,66]. The number and

size of the polymorphic inversions observed here underscores the potential importance of inversions in plant local adaptation [66]. These inversions cover ~5% of the *Zea mays* reference genome, and their role in patterning both molecular and phenotypic variation [26] among populations is significant. As even denser marker datasets become available, continued sampling of additional populations will undoubtedly reveal new, smaller, and geographically restricted inversions segregating in plant populations.

### Multiple approaches to understand local adaptation

Different approaches to identify loci conferring local adaptation yielded very different sets of candidates. Rather than indicating a lack of evidence for local adaptation, we argue that the weak correspondence between methods is reflective of biological factors including the kind of natural selection and the effects of population structure. For example, SNPs showing environmental association are only weakly correlated with  $F_{ST}$  and  $F_{CT}$  p-values (Table S3). The same observation was made for trees by Eckert et al. [67] and Keller et al. [68] who compared  $F_{ST}$  outliers to SNPs correlating with environment. Because  $F_{ST}$  outlier methods detect excess divergence among populations regardless of the distribution of environmental variation, they are likely more powerful for the identification of loci related to factors that do not correlate with measured environmental variables. All of our measured environmental variables are abiotic, and it seems likely that additional important biotic factors (e.g., herbivory, competition) would not be perfectly reflected in our environmental PCs. For example the presence of *Dalbulus maidis* leafhoppers specialized to *Zea* is thought to depend on the local abundance of

maize and proximity to bodies of water [69]. Also, Moeller and Tiffin [22] found signs of local adaptation in a single population and a locus in a study on plant immunity genes of *parviglumis*. They suggested that this was caused by localized selection pressure in herbivory. In humans, too, there is evidence that pathogen diversity may play a larger role in local adaptation than climate [70].

Population structure had a considerable effect on outlier detection in all our methods. *Parviglumis* and *mexicana* do not conform to a simple two-level hierarchical island model where gene flow between populations within subspecies would be equal. As a result, some strongly differentiated populations had undue impact on  $F_{ST}$  outliers, and our  $F_{FT}$  statistic proved to be informative about such population-specific effects. For example, SNPs specific to the isolated El Rodeo and Nabogame populations have significantly smaller  $F_{ST}$  p-values than  $F_{FT}$  outliers from other populations (Figure S20). Similarly, because of its extreme temperature and precipitation, SNPs that are strongly differentiated in Nabogame ( $F_{FT}$  outliers) have significantly higher Bayes factors for PC2 than SNPs from other *mexicana* populations (Wilcoxon rank sum test,  $p < 0.001$ , Figure S21). Such geographically restricted environmental variation has been shown to cause false positives in association studies even when population structure is taken into account [71], and may be one explanation for the observation that new advantageous mutations with narrow geographic distributions were enriched among climate-associated loci in *A. thaliana* [9].

## Material and Methods

### Sampling

Ten to twelve individuals were sampled from each of eleven populations of *parviglumis* and ten populations of *mexicana* (Figure 1, Table S7). Seeds from four populations of *parviglumis* (Ejutla A and B, San Lorenzo and La Mesa) were sampled by MBH in 2007, while the remaining 7 populations were obtained from non-regenerated bulked seed from accessions in the USDA germplasm collections. All *mexicana* populations were collected in 2008 by Pesach Lubinsky and provided by Norman Ellstrand. A *Tripsacum dactyloides* sample provided by Sherry Flint-Garcia was used as an outgroup. Geodetic distances among populations vary from 3 km between Santa Clara and Opopeo to 1503 km between El Rodeo and Nabogame, and the populations cover an altitudinal range from 590 to 2609 meters above sea level. An initial PCA that included 279 maize inbred lines [27] revealed that two *mexicana* individuals appeared to be recent hybrids with maize (Figure S24), and these were removed from subsequent analyses.

### SNP genotyping

DNA was extracted from leaf tips of seedlings at the five-leaf stage, and tissue was stored at 80°C overnight and lyophilized for 48 h. DNA was extracted from homogenized tissue following a modified CTAB protocol [72] and quantified using a NanoDrop spectrophotometer (NanoDrop Technologies, Inc., Wilmington, DE, USA) and Wallac VICTOR2 fluorescence plate reader (Perkin-Elmer Life and Analytical Sciences, Torrance, CA) with Quant-iT™ PicoGreen® dsDNA Assay Kit (Invitrogen, Grand Island, NY).

Single nucleotide polymorphism (SNP) genotyping was conducted at the UC Davis Genome Center using the MaizeSNP50 BeadChip and Infinium® HD Assay (Illumina, San Diego, CA). SNP genotypes were called using GenomeStudio V2009.1 (Illumina). After dropping SNPs with more than 10% missing data in either subspecies and manual adjustment of clustering, average call rates (the proportion of successfully called genotypes) per individual were 99% for both *parviglumis* and *mexicana*. Genotyping error estimated from three technical replicates of *parviglumis* was ~0.0015% after mismatches caused by missing data were excluded.

In total, 43,701 SNPs were called in *parviglumis* and 43,694 in *mexicana*. SNPs within a region on chromosome 8 that shows discrepancies between the physical and genetic maps were removed [73]. After removing monomorphic and duplicate SNPs and SNPs that did not map or mapped multiply to the maize reference genome (release 5b.60), the final data set consisted of 36,719 SNPs genotyped in both subspecies. SNP data, map positions, and annotations are available at [www.panzea.org](http://www.panzea.org) and [www.rilab.org](http://www.rilab.org).

### **Diversity and Population structure**

Observed ( $H_O$ ) and expected ( $H_E$ ) heterozygosity and deviation from Hardy-Weinberg equilibrium were calculated separately for each population using the 'genetics' package in R [74]. The inbreeding coefficient  $F_{IS}$  was calculated as  $(H_E - H_O)/H_E$ .

The `prcomp` function in R was used to perform principal component analysis (PCA) of SNP genotypes. The number of significant principal components was

estimated based on the Tracy-Widom distribution [75]. Individuals were assigned to groups based on significant PCs using Ward clustering via the `hclust` function of R.

Pairwise  $F_{ST}$  [76] was calculated for each pair of genetic groups using all polymorphic SNPs. The relationships between genetic, geodetic and altitudinal distance were evaluated using Mantel tests and partial Mantel tests in the R package 'vegan' [77]. The significance of correlations between pairwise genetic distances measured as  $F_{ST}/(1-F_{ST})$  and matrices of both geodetic distance and altitude differences among populations were estimated using 9999 permutations of rows and columns of the distance matrices. The partial Mantel test was used to test the effect of altitude and geodetic distance independent of each other.

Admixture and population structure were estimated using the software package STRUCTURE [78] based on genotypes at 10,000 random SNPs. Initial analyses included 279 maize inbred lines [27]. STRUCTURE was run under the admixture and correlated allele frequency model for a burn-in of 2500 iterations. Two independent runs of 20,000 MCMC iterations were performed for each value of K from 2 to 6 for analyses including maize, and for values of K from 2 to 9 for analyses including only teosinte samples. Results were inspected with STRUCTURE HARVESTER v0.6.8 [79] and visualized using DISTRUCT [80].

To test the placement of the Ahuacatitlan population relative to *mexicana* and *parviglumis*, distributions of D values [28] for three different divergence models were obtained. For each chromosome, a haplotype was sampled from each of three groups (Ahuacatitlan, *parviglumis* excluding Ahuacatitlan and *mexicana*) and the D value was calculated based on all informative sites. Sampling was repeated 1000

times to obtain the distribution of D. Homozygous SNPs from the sister genus *Tripsacum* were used to determine the ancestral state.

### Haplotype sharing and linkage disequilibrium

Haplotypes were inferred with fastPHASE [81] using known haplotypes of 18 teosinte inbred lines [49] and default parameters. Sites with residual heterozygosity were excluded. Segments of identity by state (IBS) and runs of homozygosity were identified using GERMLINE [82], with a seed segment size of 50 SNPs and allowing zero heterozygous and homozygous mismatches. Genetic map coordinates for each SNP were obtained from a modified map of the maize IBM mapping population [73]. Markers for which the genetic and physical map disagreed were omitted from haplotype based analyses.

The software TASSEL [83] was used to calculate linkage disequilibrium ( $r^2$  and p-value) using phased data from all individuals and pairs of sites with minimum allele frequency  $>0.1$ .

### Candidate SNP identification

BAYENV [29] was used to evaluate the correlation between environmental variables and allele frequencies of individual SNPs. A random set of 10,000 SNPs was used to make three covariance matrices: all populations and separately for each subspecies without the Ahuacatitlan *parviglumis* population. For each covariance matrix, two independent runs of 50,000 iterations were compared to control for convergence. Maximum differences between the two independent estimates of covariance matrices were always less than  $\sim 10\%$  of the smallest estimated covariance, indicating good convergence between runs.

A number of environmental variables were analyzed, including 8 soil variables, 19 bioclimatic variables, monthly precipitation and monthly mean, maximum and minimum temperature and altitude (Table S8). For climatic variables, 30 arc-second (~1 km) resolution climate data was downloaded from [www.worldclim.org](http://www.worldclim.org), and DIVA-GIS [84] was used to extract climate data for the population locations. Data for three key soil qualities (rooting conditions, oxygen availability to roots and workability) that varied among populations were downloaded from the Harmonized World Soil Database and data on 5 varying (cracking clays, volcanic, top soil clay, top soil sand, top soil loam) key modifier layers [85] were downloaded from [www.harvestchoice.org](http://www.harvestchoice.org). All variables were standardized to a mean of 0 and standard deviation of 1. The dimensionality of environmental data was reduced using principal component analysis (prcomp in R). The PCs that captured 95% of the variance in environments among populations were used as environmental variables for BAYENV (Tables S9-S11).

Five independent BAYENV runs with 1,000,000 iterations were used to identify associated SNPs with these PCs. SNPs were considered as candidates if they showed average Bayes factors across runs in the 99<sup>th</sup> percentile and were consistently in the 95<sup>th</sup> percentile of each run. A gene was considered as a candidate when one of the candidate SNPs was in the transcribed part of the gene.

To obtain the expected distribution of heterozygosity and the hierarchical differentiation statistics  $F_{CT}$  (among subspecies) and  $F_{ST}$  (among 20 populations, excluding Ahuacatitlan), 100,000 coalescent simulations were conducted under a



hierarchical island model of two groups of 100 demes using Arlequin [86]. The maximum expected heterozygosities for simulations were 0.5.

To identify SNPs underlying differentiation at the level of individual populations, F statistics were calculated in a hierarchical framework using the R package 'hierfstat' [87,88]. Variance components were calculated for three levels within each subspecies: population, focal, and individual. The focal component was

calculated for each population and locus, yielding  $F_{FT} = \frac{\hat{\sigma}_F^2}{\hat{\sigma}_F^2 + \hat{\sigma}_S^2 + \hat{\sigma}_I^2 + \hat{\sigma}_E^2}$ , the

proportion of total variance due to differentiation between a focal population and all

other populations, where  $\hat{\sigma}_F^2$ ,  $\hat{\sigma}_S^2$ ,  $\hat{\sigma}_I^2$  and  $\hat{\sigma}_E^2$  are the estimates of variance

between focal and other populations, among populations, among individuals and

error, respectively. Negative variance components were set to zero. For each

population, SNPs with  $F_{FT}$  values above the 99th percentile were considered

candidates.

### Trait association analysis

Association mapping tests were carried out on 278 inbred maize lines (Text S1)

from the association panel described in [31], which have been genotyped on the

Illumina MaizeSNP50 array [27] and phenotyped for 36 traits (127 trait/

environment combinations) [32]. The 51,253 SNPs with minor allele frequency

>0.05 were tested against at least one of the phenotypes. Associations were tested

using the model

$$\hat{G} = \mathbf{1}\mu + M\theta + S\beta + Zu + \varepsilon$$

where  $\hat{G}$  is the vector of the estimated genetic values of a given trait,  $\mu$  is the trait mean,  $M$  is the tested SNP,  $\theta$  is the SNP effect,  $S$  is the matrix of the panel structure as estimated by [31],  $\beta$  is the vector of structure effects,  $Z$  is an incidence matrix,  $u$  is a vector of random effects assumed to follow a distribution  $N(0, \sigma_g^2 K)$  where  $K$  is the genetic variance-covariance matrix modeled by a shared allele matrix, and  $\varepsilon$  is the model residual assumed to follow  $N(0, \sigma_\varepsilon^2 I_n)$ . Only SNPs significantly associated to a given trait with p-values  $< 0.05$  were retained for further analyses. To test whether enrichment for flowering time loci was affected by a loss of power due to correction for population structure, we also conducted association analyses for flowering time traits using a simplified model without population structure.

### Enrichment analyses

Enrichment of SNPs within inversions was inspected by ranking SNPs in each candidate list and calculating the proportion of SNPs within inversions in each candidate list. The joint effect of all inversions across all candidate lists was determined by assigning each SNP a maximum rank (more significant ranks are higher) across all candidate lists, and calculating the proportion of SNPs from inversions above the 99th quantile. Bootstrapping was used to obtain the statistical significance.

### Acknowledgements

We thank Jeff Glaubitz for SNP annotations and mapping, Lauren Sagara for technical assistance, Justin Gerke for modifying the IBM map, and Norm Ellstrand,

Pesach Lubinsky and Mark Millard (USDA-ARS GRIN) for seeds. Yaniv Brandvain, Graham Coop, John Doebley, Andrew Eckert, Torsten Günther, Joost van Heerwaarden and Peter Morrell provided useful comments on an earlier version of this manuscript.

## References

1. Grant PR, Grant BR (2002) Unpredictable evolution in a 30-year study of Darwin's finches. *Science* 296: 707-711.
2. Ford HD, Ford EB (1930) Fluctuation in numbers, and its influence on variation, in *Melitaea aurinia*, Rott. (Lepidoptera). *Ecol Entomol* 78: 345-352.
3. Clausen J, Keck DD, Hiesey WM (1940) Experimental studies on the nature of species. I. Effect of varied environments on western North American plants. Washington, D.C.: Gibson Brothers, Inc. 452 p.
4. Endler JA (1980) Natural Selection on Color Patterns in *Poecilia reticulata*. *Evolution* 34: 76-91.
5. Feder JL, Nosil P (2010) The efficacy of divergence hitchhiking in generating genomic islands during ecological speciation. *Evolution* 64: 1729-1747.
6. Le Corre V, Kremer A (2012) The genetic differentiation at quantitative trait loci under local adaptation. *Mol Ecol* 21: 1548-1566.
7. Lewontin RC, Krakauer J (1973) Distribution of gene frequency as a test of the theory of the selective neutrality of polymorphisms. *Genetics* 74: 175-195.
8. Fournier-Level A, Korte A, Cooper MD, Nordborg M, Schmitt J et al. (2011) A map of local adaptation in *Arabidopsis thaliana*. *Science* 334: 86-89.

9. Hancock AM, Brachi B, Faure N, Horton MW, Jarymowycz LB et al. (2011) Adaptation to climate across the *Arabidopsis thaliana* genome. *Science* 334: 83-86.
10. Turner TL, Bourne EC, Von Wettberg EJ, Hu TT, Nuzhdin SV (2010) Population resequencing reveals local adaptation of *Arabidopsis lyrata* to serpentine soils. *Nat Genet* 42: 260-263.
11. Eckert AJ, Bower AD, González-Martínez SC, Wegrzyn JL, Coop G et al. (2010) Back to nature: ecological genomics of loblolly pine (*Pinus taeda*, Pinaceae). *Mol Ecol* 19: 3789-3805.
12. Lauter N, Gustus C, Westerbergh A, Doebley J (2004) The inheritance and evolution of leaf pigmentation and pubescence in teosinte. *Genetics* 167: 1949-1959.
13. Wilkes HG (1967) Teosinte: the closest relative of maize. Cambridge: The Bussey Institution of Harvard University. 159 p.
14. Weber A, Clark RM, Vaughn L, Sánchez-Gonzalez J, Yu J et al. (2007) Major regulatory genes in maize contribute to standing variation in teosinte (*Zea mays* ssp. *parviglumis*). *Genetics* 177: 2349-2359.
15. Weber AL, Briggs WH, Rucker J, Baltazar BM, Sánchez-Gonzalez J et al. (2008) The genetic architecture of complex traits in teosinte (*Zea mays* ssp. *parviglumis*): new evidence from association mapping. *Genetics* 180: 1221-1232.

16. Hufford MB (2010) Genetic and ecological approaches to guide conservation of teosinte (*Zea mays* ssp. *parviglumis*), the wild progenitor of maize. Davis: University of California. 126 p.
17. Fukunaga K, Hill J, Vigouroux Y, Matsuoka Y, Sanchez G. J et al. (2005) Genetic diversity and population structure of teosinte. *Genetics* 169: 2241-2254.
18. Moeller DA, Tenaillon MI, Tiffin P (2007) Population structure and its effects on patterns of nucleotide polymorphism in teosinte (*Zea mays* ssp. *parviglumis*). *Genetics* 176: 1799-1809.
19. Smith JSC, Goodman MM, Stuber CW (1984) Variation within teosinte. III. Numerical analysis of allozyme data. *Econ Bot* 38: 97-113.
20. Doebley J, Goodman MM, Stuber CW (1987) Patterns of isozyme variation between maize and Mexican annual teosinte. *Econ Bot* 41: 234-246.
21. van Heerwaarden J, Ross-Ibarra J, Doebley J, Glaubitz JC, Sánchez González JJ et al. (2010) Fine scale genetic structure in the wild ancestor of maize (*Zea mays* ssp. *parviglumis*). *Mol Ecol* 19: 1162-1173.
22. Moeller DA, Tiffin P (2008) Geographic variation in adaptation at the molecular level: a case study of plant immunity genes. *Evolution* 62: 3069-3081.
23. Ting YC (1964) Chromosomes of maize-teosinte hybrids. Cambridge: The Bussey Institution of Harvard University. 45 p.
24. Mano Y, Omori F, Takeda K (2012) Construction of intraspecific linkage maps, detection of a chromosome inversion, and mapping of QTL for constitutive root aerenchyma formation in the teosinte *Zea nicaraguensis*. *Mol Breed* 29: 137-146.

25. Hufford MB, Xu X, van Heerwaarden J, Pyhäjärvi T, Chia J-M et al. (2012) Comparative population genomics of maize domestication and improvement. *Nat Genet* 44: 808-811.
26. Fang Z, Pyhäjärvi T, Weber AL, Dawe RK, Glaubitz JC. et al. (2012) Megabase-scale inversion polymorphism in the wild ancestor of maize. *Genetics* 191: 883-894.
27. Cook JP, McMullen MD, Holland JB, Tian F, Bradbury P et al. (2012) Genetic architecture of maize kernel composition in the nested association mapping and inbred association panels. *Plant Physiol* 158: 824-834.
28. Green RE, Krause J, Briggs AW, Maricic T, Stenzel U et al. (2010) A draft sequence of the Neandertal genome. *Science* 328: 710-722.
29. Coop G, Witonsky D, Di Rienzo A, Pritchard JK (2010) Using environmental correlations to identify loci underlying local adaptation. *Genetics* 185: 1411-1423.
30. Excoffier L, Hofer T, Foll M (2009) Detecting loci under selection in a hierarchically structured population. *Heredity* 103: 285-298.
31. Flint-Garcia SA, Thuillet AC, Yu J, Pressoir G, Romero SM et al. (2005) Maize association population: a high-resolution platform for quantitative trait locus dissection. *Plant J* 44: 1054-1064.
32. Hung H-Y, Shannon LM, Tian F, Bradbury PJ, Chen C et al. *ZmCCT* and the genetic basis of daylength adaptation underlying the post-domestication spread of maize. *Proc Natl Acad Sci USA* In Press.

33. Kato Y, Miwa K, Takano J, Wada M, Fujiwara T (2009) Highly boron deficiency-tolerant plants generated by enhanced expression of NIP5;1, a boric acid channel. *Plant Cell Physiol* 50: 58-66.
34. Horton MW, Hancock AM, Huang YS, Toomajian C, Atwell S et al. (2012) Genome-wide patterns of genetic variation in worldwide *Arabidopsis thaliana* accessions from the RegMap panel. *Nat Genet* 44: 212-216.
35. Turner TL, Von Wettberg EJ, Nuzhdin SV (2008) Genomic analysis of differentiation between soil types reveals candidate genes for local adaptation in *Arabidopsis lyrata*. *PLoS ONE* 3: e3183.
36. Smith JSC, Goodman MM, Lester RN (1981) Variation within teosinte. I. Numerical analysis of morphological data. *Econ Bot* 35: 187-203.
37. Buckler, E.S, Goodman MM, Holtsford TP, Doebley JF, Sanchez G (2006) Phylogeography of the wild subspecies of *Zea mays*. *Maydica* 51: 123-134.
38. van Heerwaarden J, Doebley J, Briggs WH, Glaubitz JC, Goodman MM et al. (2011) Genetic signals of origin, spread, and introgression in a large sample of maize landraces. *Proc Natl Acad Sci USA* 108: 1088-1092.
39. Poggio L, Rosato M, Chiavarino AM, Naranjo CA (1998) Genome size and environmental correlations in maize (*Zea mays* ssp. *mays*, Poaceae). *Ann Bot* 82: 107-115.
40. Ross-Ibarra J, Tenailon M, Gaut BS (2009) Historical divergence and gene flow in the genus *Zea*. *Genetics* 181: 1399-1413.
41. Siol M, Wright SI, Barratt SCH (2010) The population genomics of plant adaptation. *New Phytol* 188: 313-332.

42. Städler T, Haubold B, Merino C, Stephan W, Pfaffelhuber P (2009) The impact of sampling schemes on the site frequency spectrum in nonequilibrium subdivided populations. *Genetics* 182: 205-216.
43. De A, Durrett R (2007) Stepping-stone spatial structure causes slow decay of linkage disequilibrium and shifts the site frequency spectrum. *Genetics* 176: 969-981.
44. St. Onge KR, Palmé AE, Wright SI, Lascoux M (2012) Impact of sampling schemes on demographic inference: an empirical study in two species with different mating systems and demographic histories. *G3* 2: 803-814.
45. Hancock AM, Witonsky DB, Alkorta-Aranburu G, Beall CM, Gebremedhin A et al. (2011) Adaptations to climate-mediated selective pressures in humans. *PLoS Genet* 7: e1001375.
46. Schnable PS, Ware D, Fulton RS, Stein JC, Wei F et al. (2009) The B73 maize genome: complexity, diversity, and dynamics. *Science* 326: 1112-1115.
47. Studer A, Zhao Q, Ross-Ibarra J, Doebley J (2011) Identification of a functional transposon insertion in the maize domestication gene *tb1*. *Nat Genet* 43: 1160-1163.
48. Salvi S, Sponza G, Morgante M, Tomes D, Niu X et al. (2007) Conserved noncoding genomic sequences associated with a flowering-time quantitative trait locus in maize. *Proc Natl Acad Sci USA* 104: 11376-11381.
49. Chia J-M, Song C, Bradbury P, Costich D, de Leon N et al. (2012) Capturing extant variation from a genome in flux: maize HapMap II. *Nat Genet* 44: 803-807.



50. Iltis HH, Doebley JF (1980) Taxonomy of *Zea* (Gramineae). II. Subspecific categories in the *Zea mays* complex and a generic synopsis. *Am J Bot* 67: 994-1004.
51. Olsson K, Ågren J (2002) Latitudinal population differentiation in phenology, life history and flower morphology in the perennial herb *Lythrum salicaria*. *J Evol Biol* 15: 983-996.
52. Lowry DB, Rockwood RC, Willis JH (2008) Ecological reproductive isolation of coast and inland races of *Mimulus guttatus*. *Evolution* 62: 2196-2214.
53. Galinat WC (1967) Plant habit and the adaptation of corn. *Mass Agric Exp Stn Bull* 565: 1-16.
54. Chalker-Scott L (1999) Environmental significance of anthocyanins in plant stress responses. *Photochem Photobiol* 70: 1-9.
55. Doebley J, Stec A, Hubbard L (1997) The evolution of apical dominance in maize. *Nature* 386: 485-488.
56. Jackson D, Hake S (1999) Control of phyllotaxy in maize by the *abphyl1* gene. *Development* 126: 315-323.
57. Sheldon E, Ferl R, Fedoroff N, Curtis Hannah L (1983) Isolation and analysis of a genomic clone encoding sucrose synthetase in maize: evidence for two introns in Sh. *Mol Gen Genet* 190: 421-426.
58. Kato Y. TA (1975) Cytological studies of maize (*Zea mays* L.) and teosinte (*Zea mexicana* (Schradler) Kuntze) in relation to their origin and evolution. Amherst: University of Massachusetts. 253 p.

59. Doyle GG (1994) Inversions and list of inversions available. In: Freeling M, Walbot V, editors. The Maize Handbook. New York: Springer-Verlag. pp. 346-349.
60. Kirkpatrick M, Barton N (2006) Chromosome inversions, local adaptation and speciation. *Genetics* 173: 419-434.
61. Lowry DB, Willis JH (2010) A widespread chromosomal inversion polymorphism contributes to a major life-history transition, local adaptation, and reproductive isolation. *PLoS Biol* 8: e1000500.
62. Huynh LY, Maney DL, Thomas JW (2010) Chromosome-wide linkage disequilibrium caused by an inversion polymorphism in the white-throated sparrow (*Zonotrichia albicollis*). *Heredity* 106: 537-546.
63. Cheng C, White BJ, Kamdem C, Mockaitis K, Costantini C et al. (2012) Ecological genomics of *Anopheles gambiae* along a latitudinal cline in Cameroon: a population resequencing approach. *Genetics* 190: 1417-1432.
64. Etges WJ, Levitan M (2004) Palaeoclimatic variation, adaptation and biogeography of inversion polymorphisms in natural populations of *Drosophila robusta*. *Biol J Linn Soc* 81: 395-411.
65. Dobzhansky TG (1970) *Genetics of the evolutionary process*. New York: Columbia University Press.
66. Kirkpatrick M (2010) How and why chromosome inversions evolve. *PLoS Biology* 8: e1000501.
67. Eckert AJ, van Heerwaarden J, Wegrzyn JL, Nelson CD, Ross-Ibarra J et al. (2010) Patterns of population structure and environmental associations to

aridity across the range of loblolly pine (*Pinus taeda* L., Pinaceae). *Genetics* 185: 969-982.

68. Keller SR, Levens N, Olson MS, Tiffin P Local adaptation in the flowering time gene network of balsam poplar, *Populus balsamifera* L. *Mol Biol Evol*: In press.
69. Medina RF, Reyna SM, Bernal JS (2012) Population genetic structure of a specialist leafhopper on *Zea*: likely anthropogenic and ecological determinants of gene flow. *Entomol Exp Appl* 142: 223-235.
70. Fumagalli M, Sironi M, Pozzoli U, Ferrer-Admetlla A, Pattini L et al. (2011) Signatures of environmental genetic adaptation pinpoint pathogens as the main selective pressure through human evolution. *PLoS Genet* 7: e1002355.
71. Mathieson I, McVean G (2012) Differential confounding of rare and common variants in spatially structured populations. *Nat Genet* 44: 243-246.
72. Saghai-Marroof MA, Soliman KM, Jorgensen RA, Allard RW (1984) Ribosomal DNA spacer-length polymorphisms in barley: Mendelian inheritance, chromosomal location, and population dynamics. *Proc Natl Acad Sci USA* 81: 8014-8018.
73. Ganai MW, Durstewitz G, Polley A, Bérard A, Buckler, E.S et al. (2011) A large maize (*Zea mays* L.) SNP genotyping array: development and germplasm genotyping, and genetic mapping to compare with the B73 reference genome. *PloS ONE* 6: e28334.
74. R Development Core Team (2010) R: A language and environment for statistical computing. Vienna: R Foundation for Statistical Computing, Vienna, Austria.

75. Patterson N, Price AL, Reich D (2006) Population structure and eigenanalysis. *PLoS Genet* 2: e190.
76. Weir BS, Cockerham CC (1984) Estimating F-statistics for the analysis of population structure. *Evolution* 38: 1358-1370.
77. Oksanen J, Blanchet GF, Kindt R, Legendre p, O'Hara RB, et al. (2011) vegan: Community Ecology Package. R package version 1.17-6. <http://CRANR-projectorg/package=vegan>.
78. Falush D, Stephens M, Pritchard JK (2003) Inference of population structure using multilocus genotype data: linked loci and correlated allele frequencies. *Genetics* 164: 1567-1587.
79. Earl, DA vonHoldt BM (2012) STRUCTURE HARVESTER: a website and program for visualizing STRUCTURE output and implementing the Evanno method. *Conserv Genet Resour* 4: 359-361.
80. Rosenberg NA (2004) DISTRUCT: a program for the graphical display of population structure. *Mol Ecol Notes* 4: 137-138.
81. Scheet P, Stephens M (2006) A fast and flexible statistical model for large-scale population genotype data: applications to inferring missing genotypes and haplotypic phase. *Am J Hum Genet* 78: 629-644.
82. Gusev A, Lowe JK, Stoffel M, Daly MJ, Altshuler D et al. (2009) Whole population, genome-wide mapping of hidden relatedness. *Genome Res* 19: 318-326.

83. Bradbury PJ, Zhang Z, Kroon DE, Casstevens TM, Ramdoss Y et al. (2007) TASSEL: software for association mapping of complex traits in diverse samples. *Bioinformatics* 23: 2633-2635.
84. Hijmans RJ, Guarino L, Cruz M, Rojas E (2001) Computer tools for spatial analysis of plant genetic resources data: 1. DIVA-GIS. *Plant Genet Resour Newsl* 127: 15-19.
85. Sanchez PA, Palm CA, Buol SW (2003) Fertility capability soil classification: a tool to help assess soil quality in the tropics. *Geoderma* 114: 157-185.
86. Excoffier L, Lischer HEL (2010) Arlequin suite ver 3.5: a new series of programs to perform population genetics analyses under Linux and Windows. *Mol Ecol Resour* 10: 564-567.
87. Goudet J (2005) HIERFSTAT, a package for R to compute and test hierarchical F-statistics. *Mol Ecol Notes* 5: 184-186.
88. Yang RC (1998) Estimating hierarchical F-statistics. *Evolution* 950-956.

## Figure legends

**Figure 1. Map of sampled *Zea mays* ssp. *parviglumis* and ssp. *mexicana* populations.**

**Figure 2. Diversity statistics.** A. Proportion of SNPs deviating from Hardy-Weinberg Equilibrium (HWE), proportion of polymorphic SNPs, and mean inbreeding coefficient  $F_{IS}$ . B. Length and number of runs of homozygosity (ROH) and average pairwise length of genomic segments identical by state (IBS).

**Figure 3. Linkage disequilibrium reveals structural rearrangements in teosinte.** Shown are linkage disequilibrium ( $r^2$ , red) and permutation p-value (black) for pairs of SNPs across chromosomes 1, 4 and 9. Dashed black lines delineate the likely boundaries of structural variants discussed in the text.

**Figure 4. Population structure in teosinte.** A. Principal component analysis of all individuals, labeled according to the sampled population. B. STRUCTURE results for all individuals. Individuals are grouped by population, and populations ordered by increasing altitude.

**Figure 5. Overlap among methods for detecting local adaptation.** Shown is the joint distribution of heterozygosity and  $F_{ST}$  under a hierarchical island model (grey dots) The red line indicates the 1 % tail of  $F_{ST}$  based on simulations. A. SNPs that have Bayes factors higher than 400 for PC2 are shown in black. B. SNPs that have a significant  $F_{FT}$  value in each population (populations are colored as in Figure 3.).

**Figure 6. Association and differentiation in teosinte.** Values are plotted across all 10 chromosomes, with each chromosome plotted in a different color. Black dots represent SNPs considered to be outliers, and black horizontal bars below the plots indicate the positions of inversions in each graph. A. Bayes factors for PC1 in *mexicana*. B.  $F_{ST}$  across 20 populations C.  $F_{CT}$  between subspecies.

## Supporting information captions

**Figure S1.** Distribution of total expected heterozygosity within *parviglumis* and *mexicana* across all loci.

**Figure S2.** Runs of homozygosity across all 10 chromosomes. Each individual is one horizontal line in the graph. Populations are separated by colors.

**Figure S3.** LD in chromosome 9 among *mexicana* populations based on SNPs with minor allele frequency >0.1

**Figure S4.** Neighbor-joining tree for *Inv1n* based on percentage of SNPs differing among haplotypes. SNPs with missing data were excluded from pairwise comparisons. The tree was rooted based on *Tripsacum*. Red: *parviglumis*, orange, *mexicana*, green: maize, purple: *Tripsacum*. Black branches indicate the inverted haplotype.

**Figure S5.** Neighbor-joining tree for *Inv4m* based on percentage of SNPs differing among haplotypes. SNPs with missing data were excluded from pairwise comparisons. The tree was rooted based on *Tripsacum*. Red: *parviglumis*, orange, *mexicana*, green: maize, purple: *Tripsacum*. Black branches indicate the inverted haplotype.

**Figure S6.** Neighbor-joining tree for *Inv9d* based on percentage of SNPs differing among haplotypes. SNPs with missing data were excluded from pairwise comparisons. The tree was rooted based on *Tripsacum*. Red: *parviglumis*, orange, *mexicana*, green: maize, purple: *Tripsacum*. Black branches indicate the inverted haplotype.

**Figure S7.** Neighbor-joining tree for *Inv9e* based on percentage of SNPs differing among haplotypes. SNPs with missing data were excluded from pairwise comparisons. The tree was rooted based on *Tripsacum*. Red: *parviglumis*, orange, *mexicana*, green: maize, purple: *Tripsacum*. Black branches indicate the inverted haplotype. Black dashed outer lines indicate parts of the tree that are putatively part of the inverted group.

**Figure S8.** The proportion of individuals sharing IBD segments with *parviglumis* (red) or *mexicana* (orange) for each *parviglumis* population along the genome, scaled in genetic distance. Within population and within individual comparisons are excluded. Numbers on the x-axis indicate chromosome midpoints. Total length of the genetic map is ~3700 cM.

**Figure S9.** The proportion of individuals sharing IBD segments with *parviglumis* (red) or *mexicana* (orange) for each *mexicana* population along the genome scaled in genetic distance. Within population and within individual comparisons are



excluded. Numbers on the x-axis indicate chromosome midpoints. Total length of the genome is ~3700 cM.

**Figure S10.** Altitudinal clines of three inversions presented as a relationship between altitude and haplotype distance within each inversion. Distance (as a number of SNPs for which they differ) of each haplotype from the most distal haplotype in the main low diversity haplotype group is in the y-axis. Colors indicate populations. A. *Inv1n*, B. *Inv4m* and C. *Inv9d*.

**Figure S11.** Third and fourth principal component from PCA on *parviglumis* and *mexicana*.

**Figure S12.** Structure results for joint analysis of 130 *parviglumis*, 120 *mexicana* and 279 maize lines for K values 2-6, based on 20 000 iterations with a 2500 step burn-in. Colors represent each individual's proportion of ancestry in each genetic group.

**Figure S13.** Dendrogram based on Ward clustering of individuals using the first 20 PCs. Red dashed line indicates the segment that divides individuals into 21 groups.

**Figure S14.** Isolation by geodetic and altitudinal distance among all populations and within both subspecies. Geodetic or altitudinal distance on y-axis and genetic differentiation on x-axis. P-values are from Mantel (A-C) and partial Mantel tests (A),

where correlation with both geodetic and altitude was conditioned on the other variable.

**Figure S15.** Distribution of D values for three possible divergence scenarios of Ahuacatitlan population, *parviglumis* and *mexicana*. The center of expected distribution (0) is marked with vertical dashed line.

**Figure S16.** Natural logarithm of Bayes factors for each of six PCs along chromosomes for the joint analysis of 20 *parviglumis* and *mexicana* populations. Inversions are marked as horizontal segments.

**Figure S17.** Natural logarithm of Bayes factors for each of four PCs along chromosomes for the analysis of 10 *parviglumis* populations. Inversions are marked as horizontal segments.

**Figure S18.** Natural logarithm of Bayes factors for each four PCs along chromosomes for the analysis of 10 *mexicana* populations. Inversions are marked as horizontal segments.

**Figure S19.** Joint distribution of heterozygosity with  $F_{CT}$  (A) and  $F_{ST}$  (B) under a hierarchical model. Black lines indicate 1% cutoff based on simulations. The six SNPs investigated in detail are shown in red.

**Figure S20.** Boxplot of p-value distribution for  $F_{ST}$  outliers for all SNPs (All) and for SNPs that are  $F_{FT}$  outliers in each population.

**Figure S21** Boxplot of the logarithm of Bayes factors for PC2 among *mexicana* populations for all SNPs (All) and for SNPs that are  $F_{FT}$  outliers in each *mexicana* population.

**Figure S22.** Diversity and environmental association along *mexicana* chromosome 9. A) Per SNP expected heterozygosity  $H_E$ . Darker lines indicate higher elevation populations. B) Natural logarithm of Bayes factors for PC1. Candidate SNPs for PC1 are indicated as black circles.

**Figure S23.** Neighbour-joining tree based on pairwise  $F_{ST}$  among groups identified by PCA.

**Figure S24.** Principal component analysis of 130 *parviglumis*, 120 *mexicana* and 279 maize lines based on 37,021 SNPs. Two outlier *mexicana* individuals are likely recent hybrids between maize and *mexicana*.

**Table S1.** Summary statistics of genetic diversity for each population.

**Table S2.** Candidate status for each 36,719 SNPs in filtered dataset. Marker: marker name at panzea.org, Locus: Original SNP name, Chr: chromosome, Pos: B73

RefGen\_v2 position (bp), Type: annotation for SNPs in coding regions. Column names indicate different candidate sets. TRUE: the SNP is a candidate, FALSE: the SNP is not a candidate, NA: the SNP was not included in the analysis.

**Table S3.** Spearman's correlation between Bayes factors and p-values for  $F_{CT}$  and  $F_{ST}$ .

**Table S4.** Enrichment of functional properties among candidate SNPs and genes.

**Table S5.** Enrichment of SNPs that are associated with a maize phenotypic trait for each list of adaptation candidates. GWAS was done using a mixed linear model that takes both population structure and relatedness into account.

**Table S6.** Enrichment of SNPs that are associated with a maize phenotypic trait for each list of adaptation candidates. GWAS was done using a simple model not taking population structure into account.

**Table S7.** Information about sampled populations ordered by ascending altitude.

**Table S8.** Environmental variables and abbreviations used in the study.

**Table S9.** Variable loadings/rotations for each of 6 PCs that were used in BAYENV for the joint dataset of 20 *parviglumis* and *mexicana* populations.

**Table S10.** Variable loadings/rotations for each of 4 PCs that were used in BAYENV for 10 *parviglumis* populations

**Table S11.** Variable loadings/rotations for each of 4 PCs that were used in BAYENV for 10 *mexicana* populations

**Text S1.** List of 278 maize inbred lines used in the association analysis

## Tables

**Table 1. Summary of environmental correlation and differentiation outlier results.**

<b>Analysis</b>	<b>Variable</b>	<b>Major loadings</b>	<b>BF, 99th<sup>a</sup></b>	<b>No. cand SNPs</b>	<b>No. cand genes</b>
Both	PC1	altitude, temperature	116.8	262	162
	PC2	temperature seasonality, soil quality and precipitation	400.0	359	222
	PC3	precipitation	40.4	308	201
	PC4	topsoil variables and precipitation seasonality	39.4	229	145
	PC5	mean diurnal range of temperature plus some soil variables	72.9	291	184
	PC6	mean diurnal range of temperature plus some soil variables	10.2	225	151
<i>parviglumis</i>	PC1	altitude, temperature	2.2	60	36
	PC2	temperature range and seasonality	6.4	173	118
	PC3	soil type and precipitation	2.0	102	69
	PC4	monthly precipitation and mean diurnal range of temperature	4.8	42	24
<i>mexicana</i>	PC1	altitude, temperature	6.9	108	69
	PC2	temperature seasonality and range and precipitation.	52.3	309	204
	PC3	precipitation and volcanic soil	31.1	27	16
	PC4	top soil variables and temperature variability	3.8	93	58
F <sub>CT</sub>				731	728
F <sub>ST</sub>				1363	411

<sup>a</sup> Bayes factor at 99th percentile of distribution

**Table 2. Enrichment of sets of candidate SNPs within four inversions.**

Analysis	Variable	p-value				
		<i>Inv1n</i>	<i>Inv4m</i>	<i>Inv9d</i>	<i>Inv9e</i>	All inversions
Both	PC1	<0.001 (4.5)	0.003 (3.7)	<0.001 (7.6)	0.027 (2.2)	0.0001 (3.3)
	PC2	0.032 (1.7)	0.824	<0.001 (3.9)	0.331	0.0016 (1.8)
	PC3	<0.001 (5.7)	1.000	0.819	0.186	0.0001 (2.2)
	PC4	0.002 (2.7)	0.574	0.001 (3.1)	<0.001 (4.0)	0.0001 (2.5)
	PC5	0.440	1.000	1.000	0.938	0.9942
	PC6	0.672	1.000	0.859	0.687	0.9745
<i>parviglumis</i>	PC1	0.450	1.000	0.290	1.000	0.0181 (1.5)
	PC2	0.616	0.016 (3.2)	0.045 (2.3)	0.728	0.1555
	PC3	0.261	1.000	1.000	0.812	0.3764
	PC4	0.271	1.000	1.000	0.474	0.4543
<i>mexicana</i>	PC1	0.001 (3.8)	1.000	<0.001 (33.0)	0.095	0.0001 (3.2)
	PC2	0.748	0.694	<0.001 (4.3)	0.027 (2.0)	0.0007 (1.8)
	PC3	0.136	1.000	1.000	1.000	0.799
	PC4	0.002 (3.9)	1.000	1.000	<0.001 (8.2)	0.0001 (2.0)
F <sub>CT</sub>		<0.001 (2.9)	<0.001 (11.7)	0.049 (1.6)	0.705	0.0001 (3.4)
F <sub>ST</sub>		<0.001 (2.7)	<0.001 (6.3)	<0.001 (1.8)	0.866	0.0001 (3.2)

For each p-value < 0.05 the fold enrichment is reported in parenthesis. P-values are based on bootstrapping.

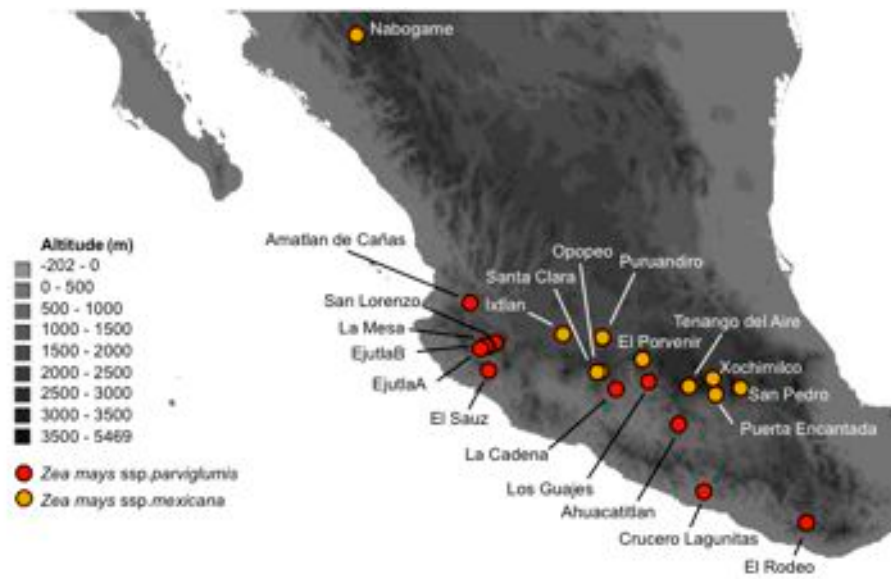


Figure 1



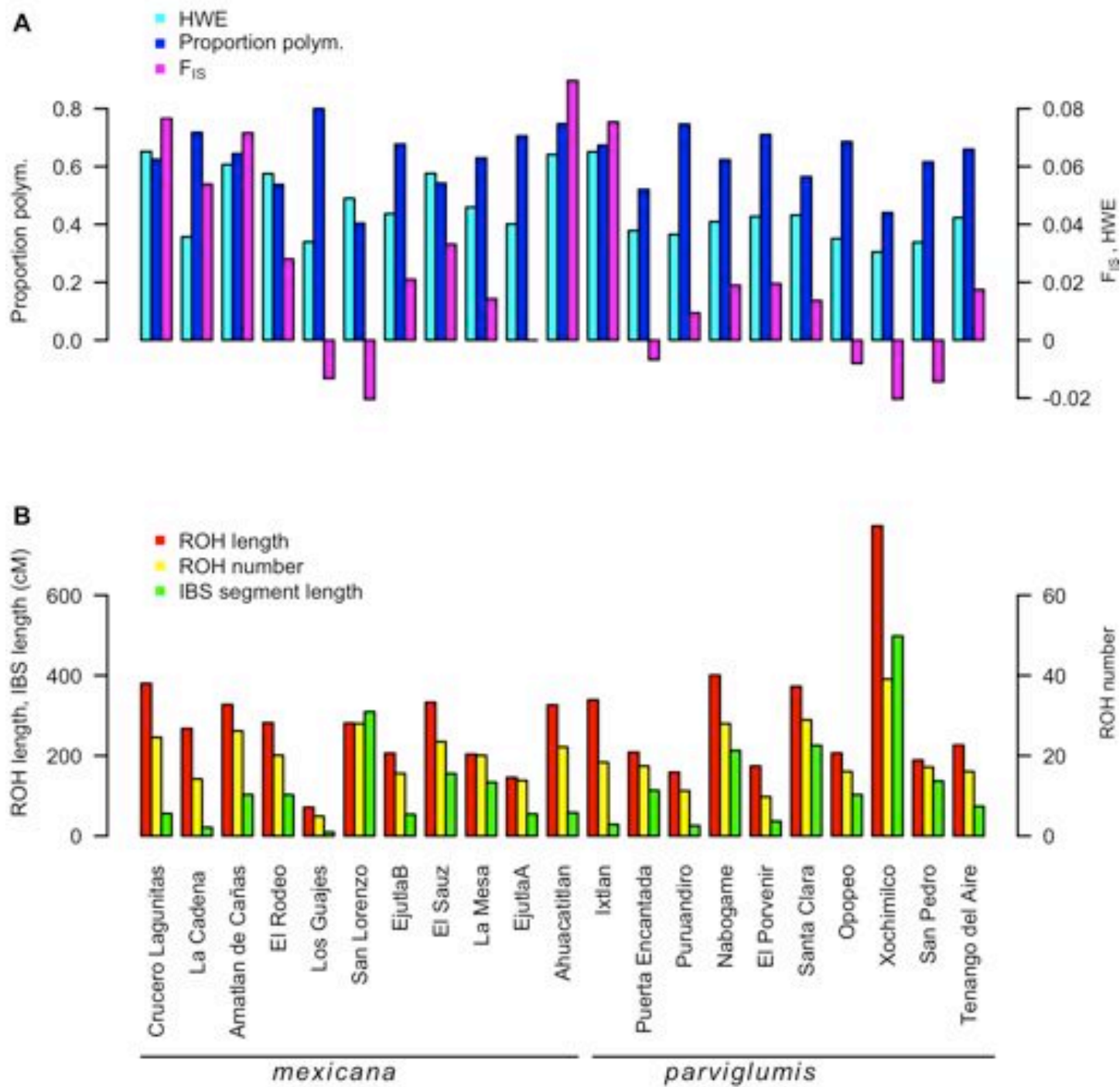


Figure 2

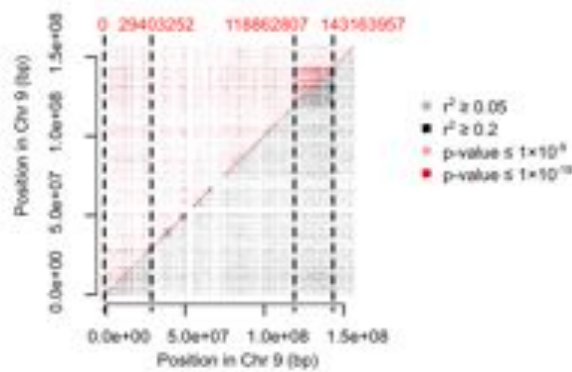
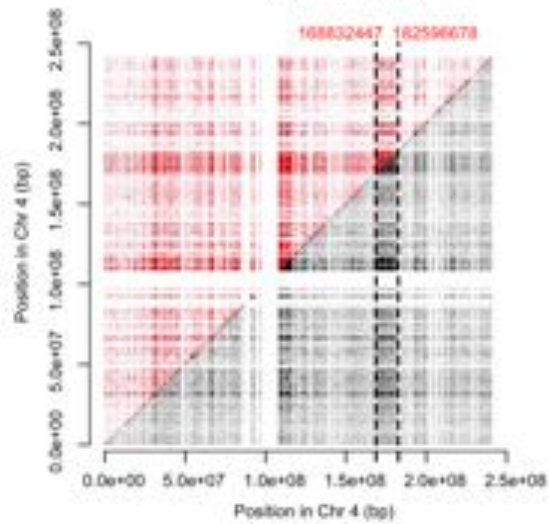
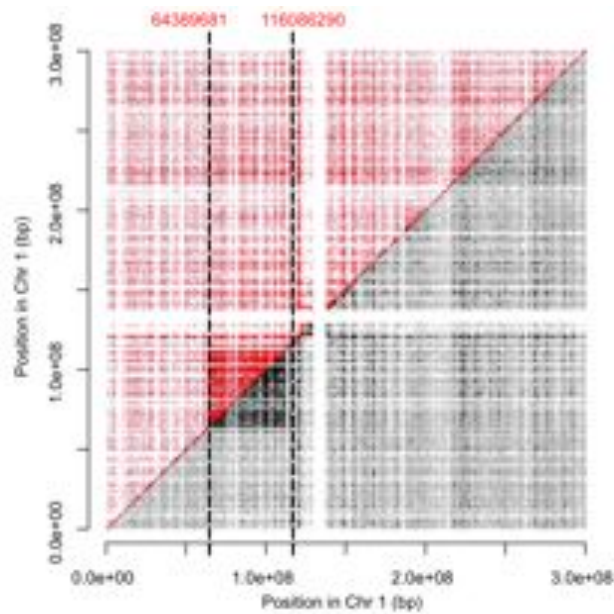


Figure 3

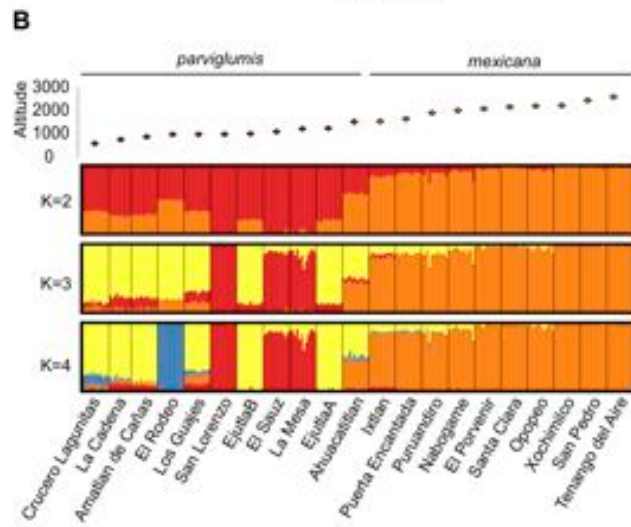
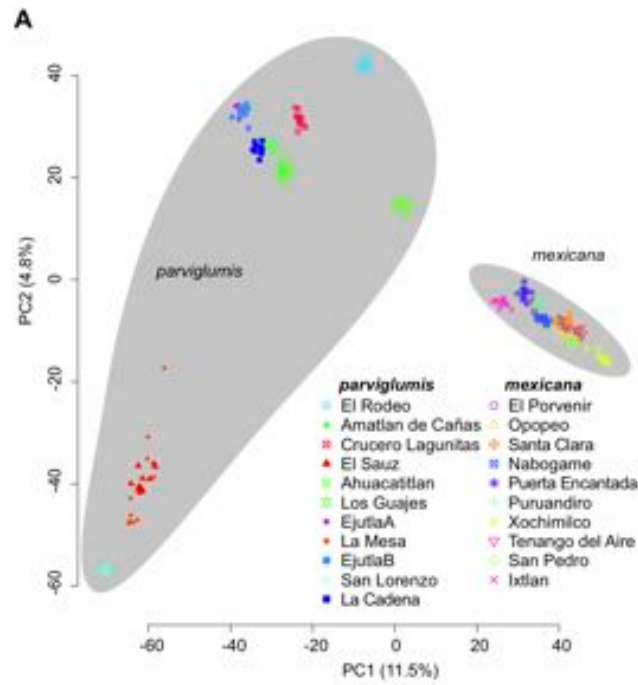


Figure 4

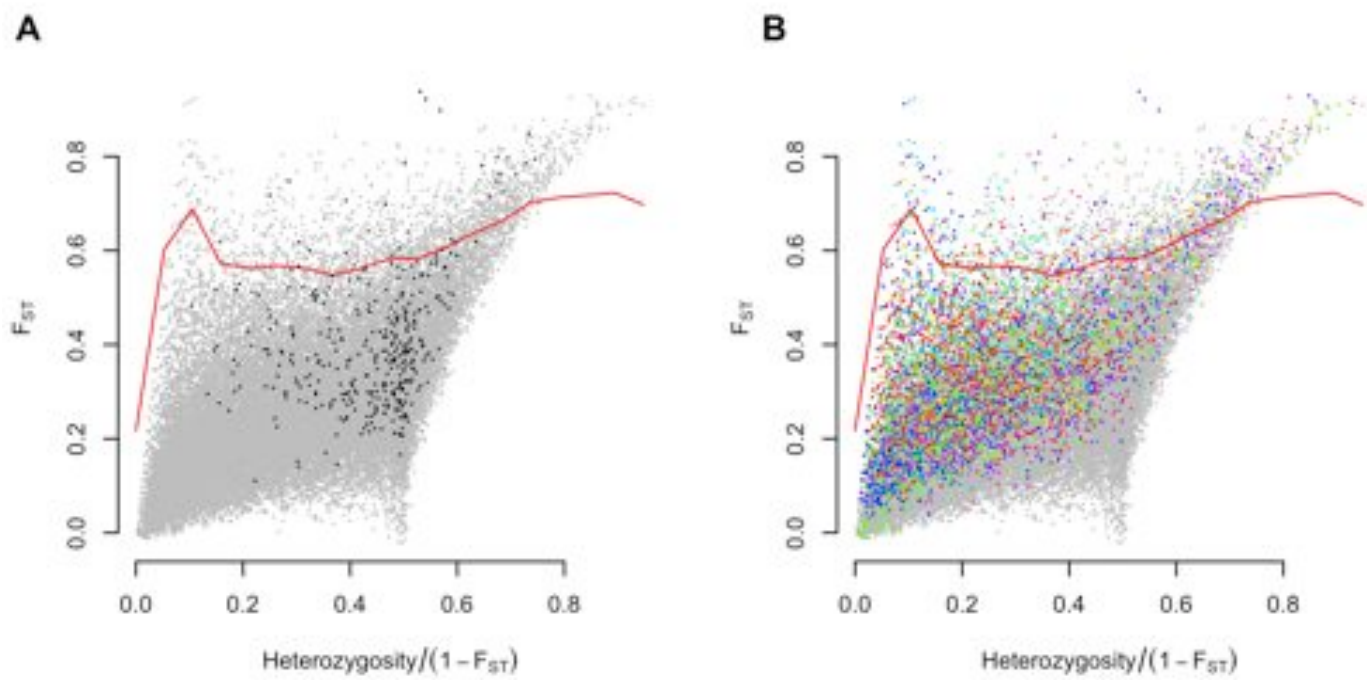


Figure 5

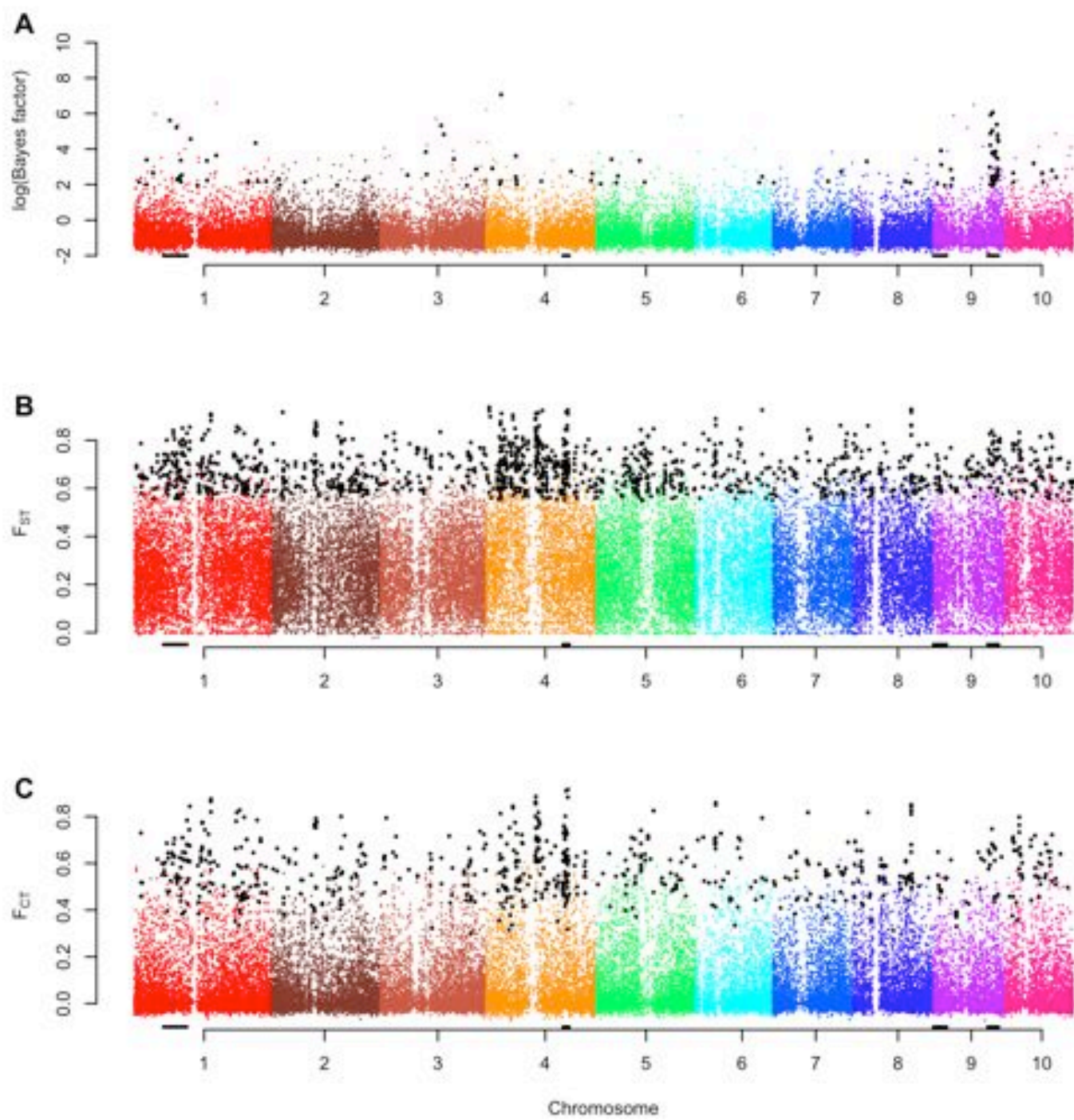


Figure 6

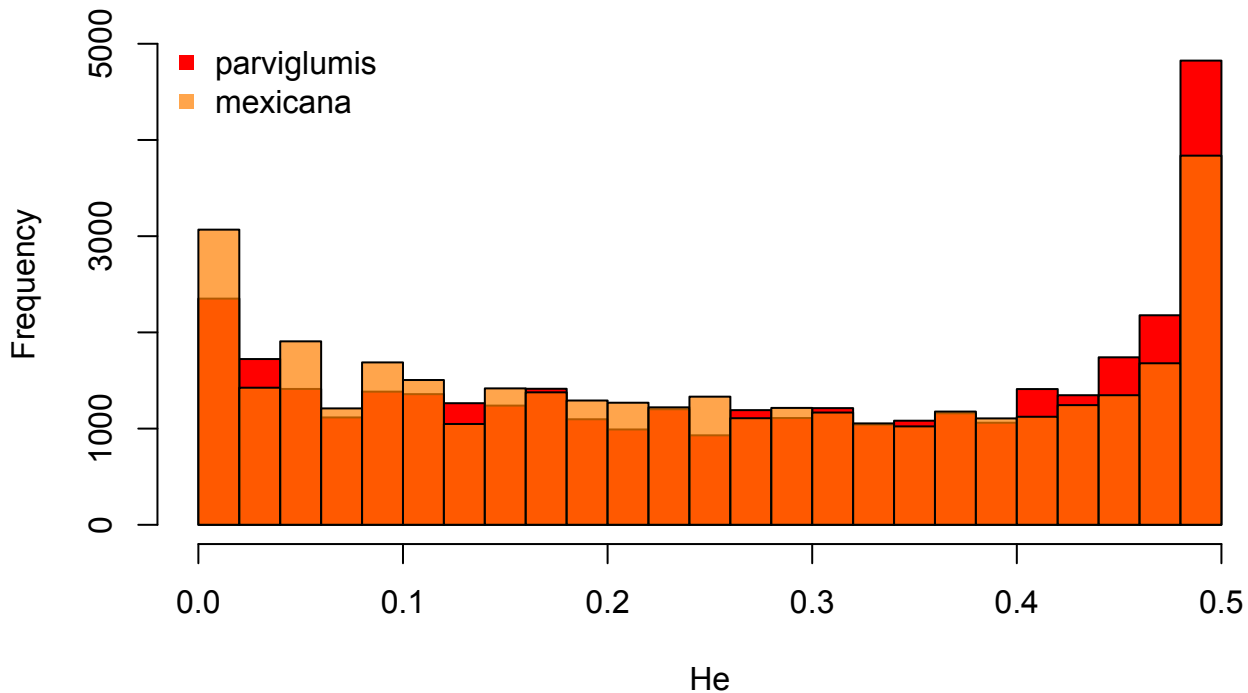


Figure S1

# Runs of homozygosity

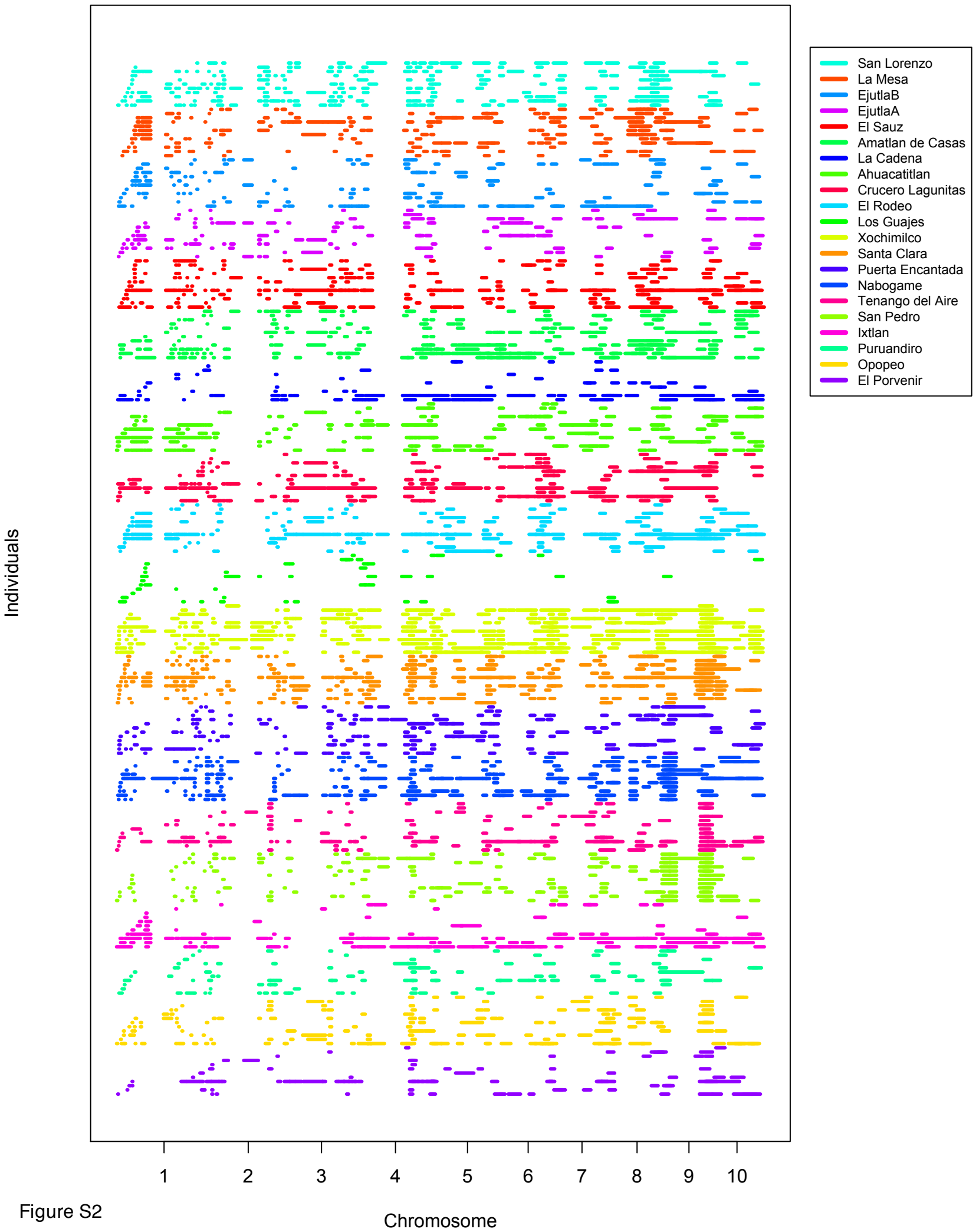


Figure S2

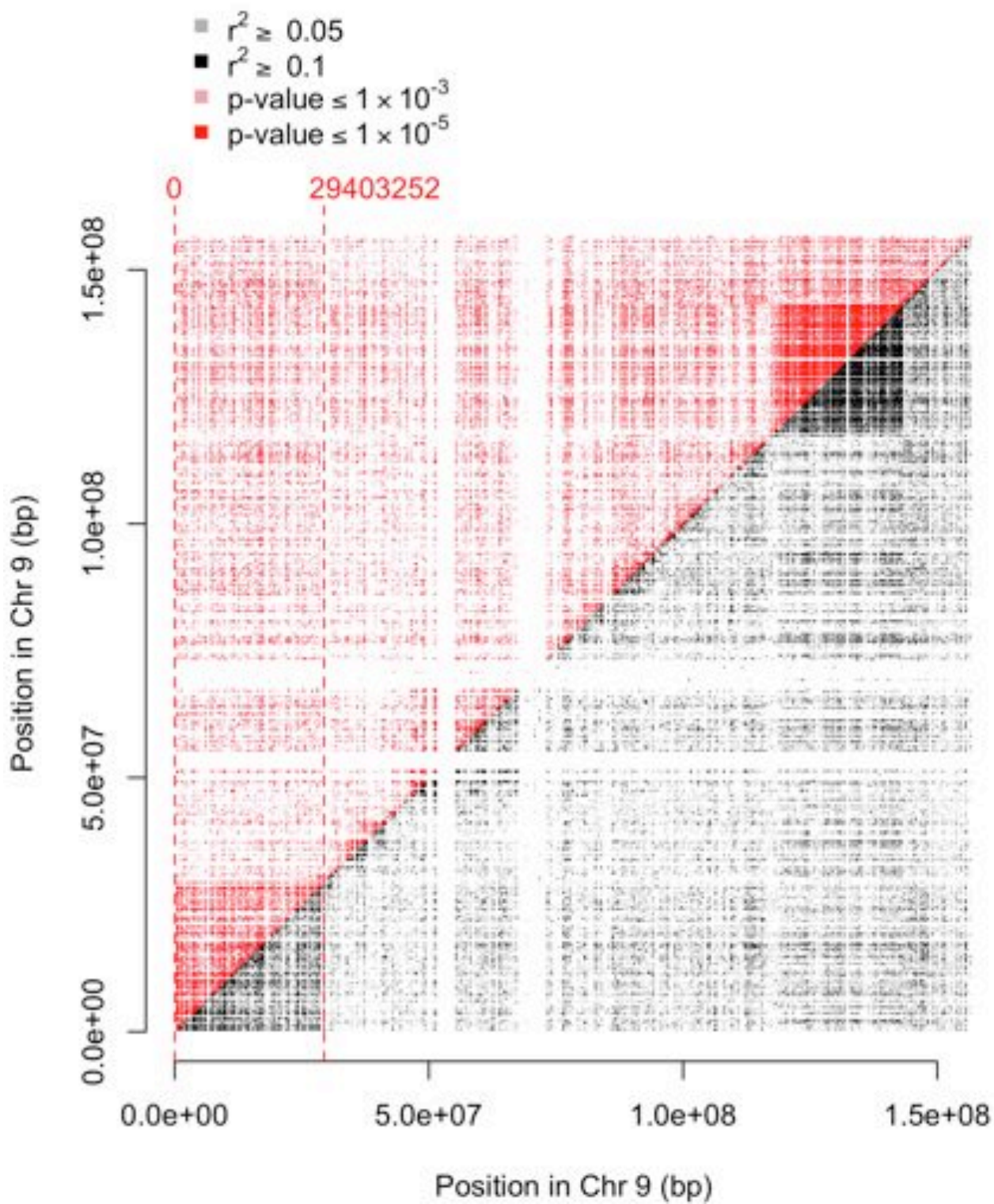


Figure S3



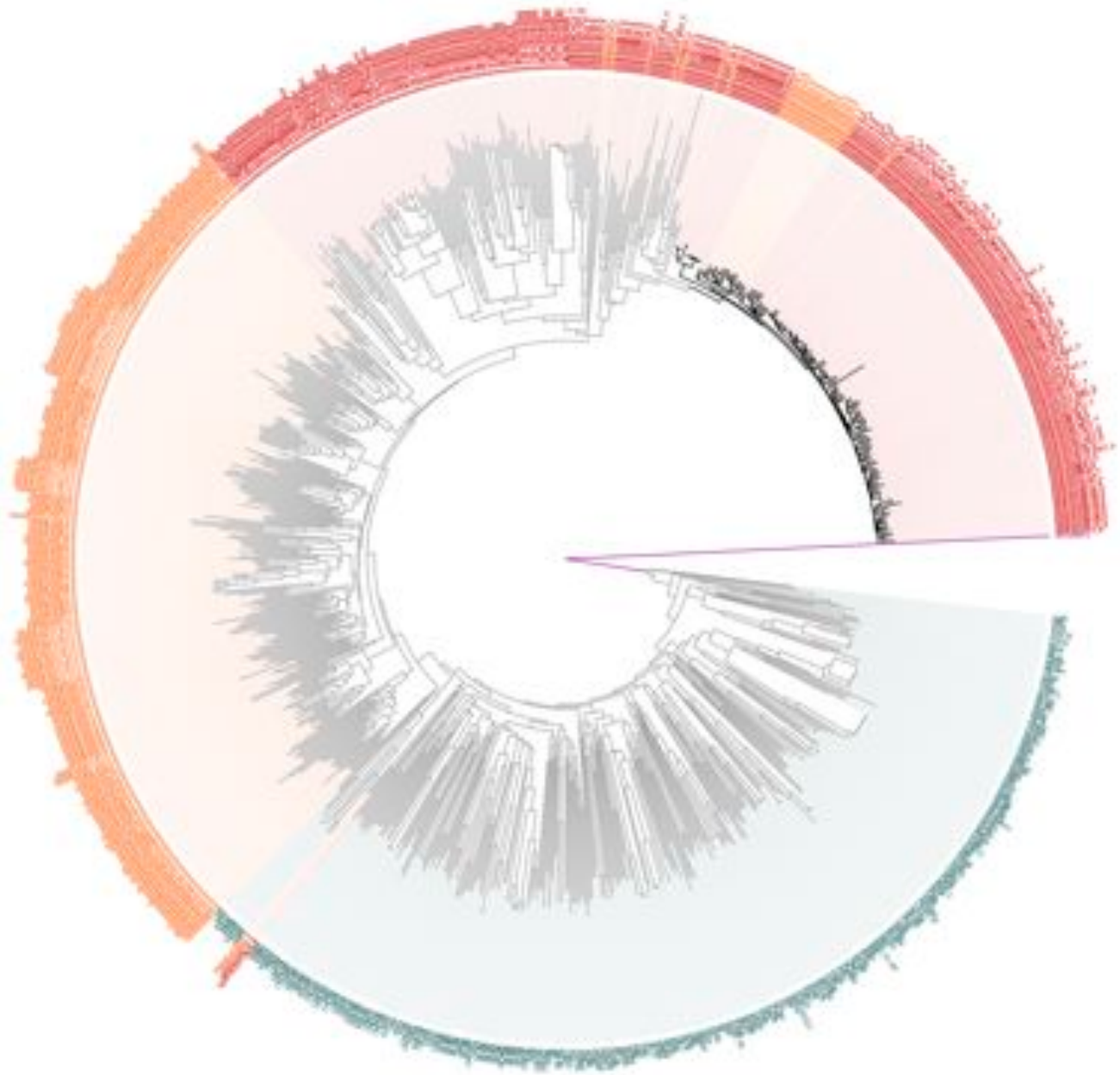


Figure S4

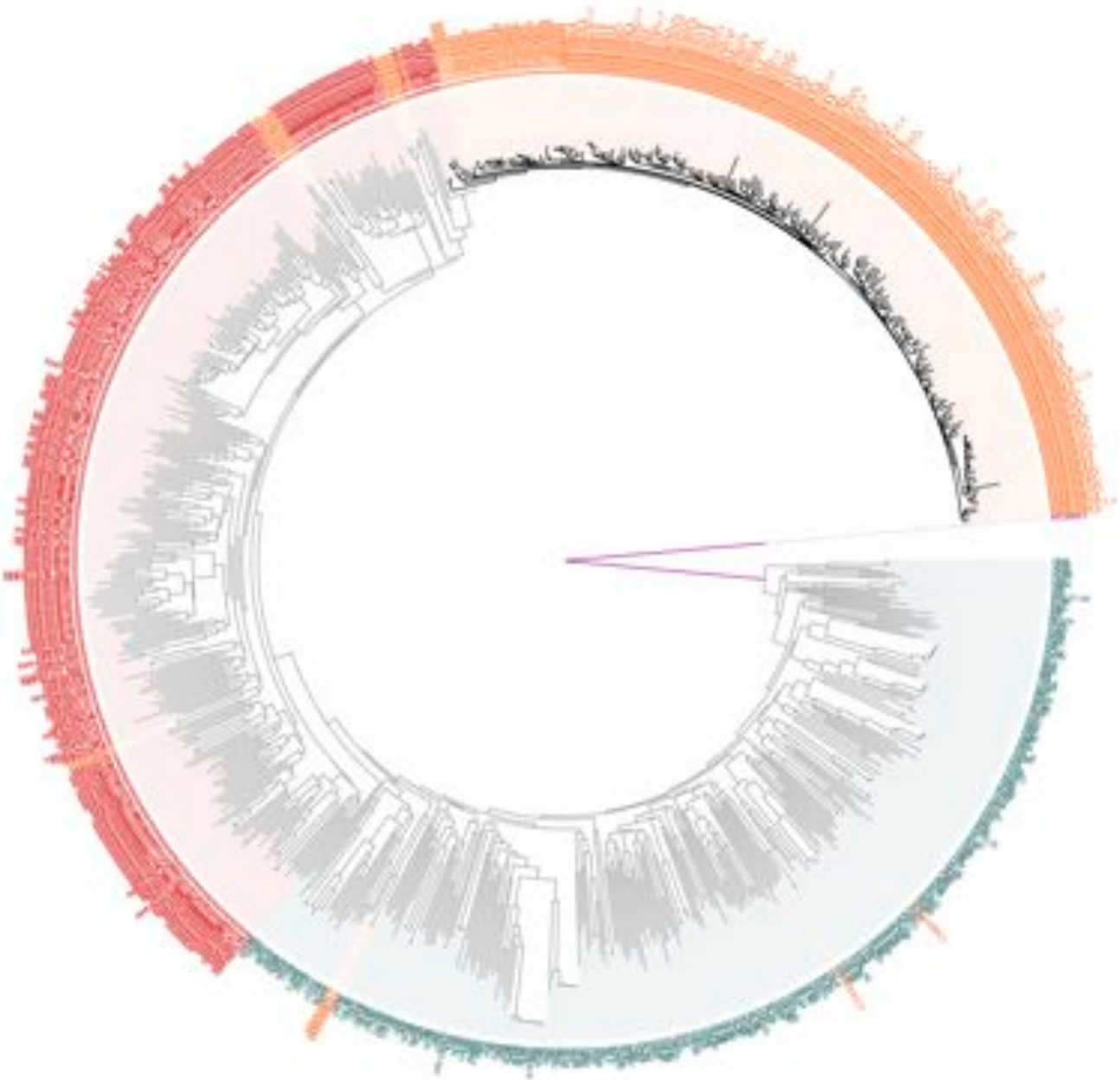


Figure S5

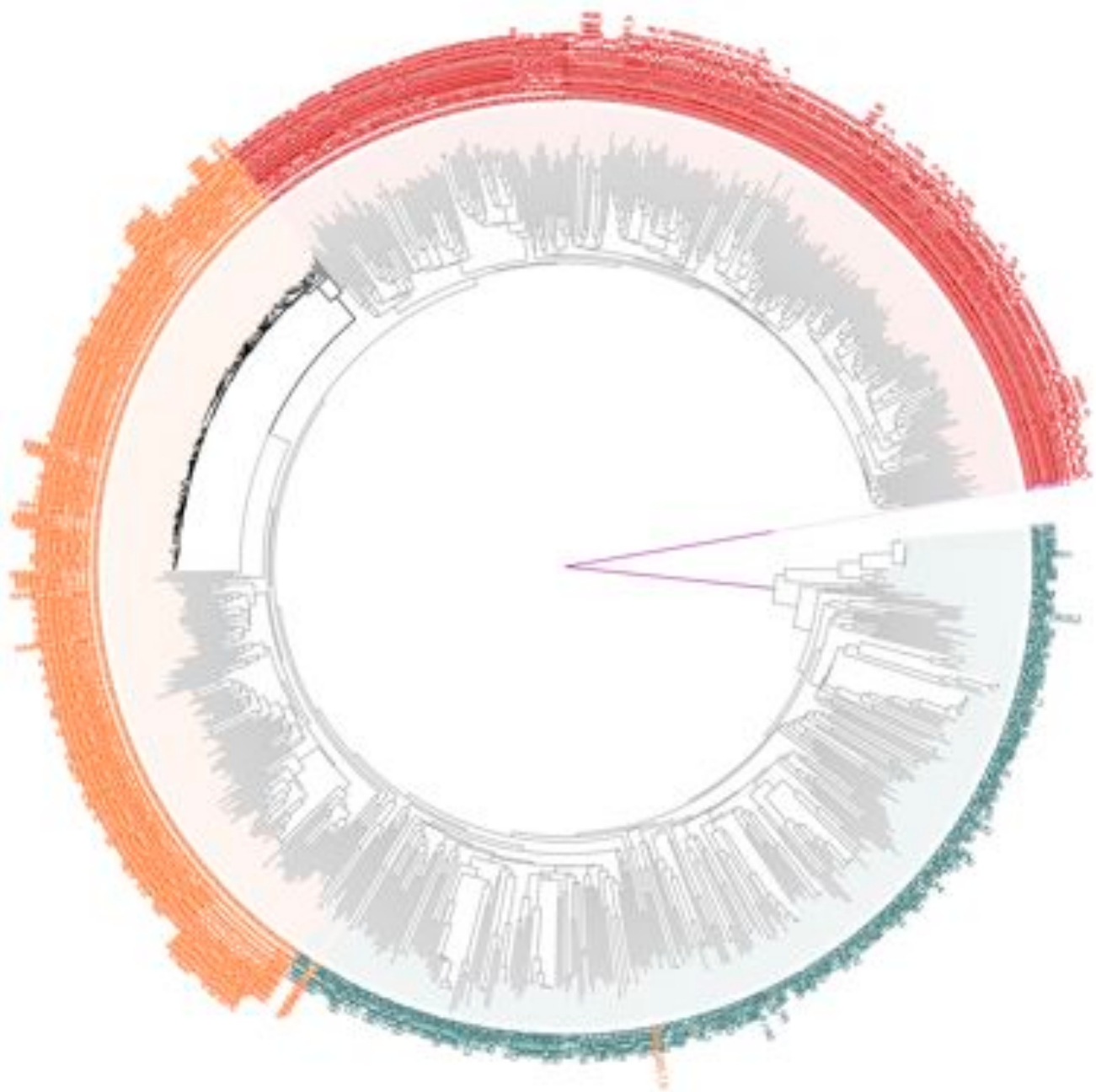


Figure S6

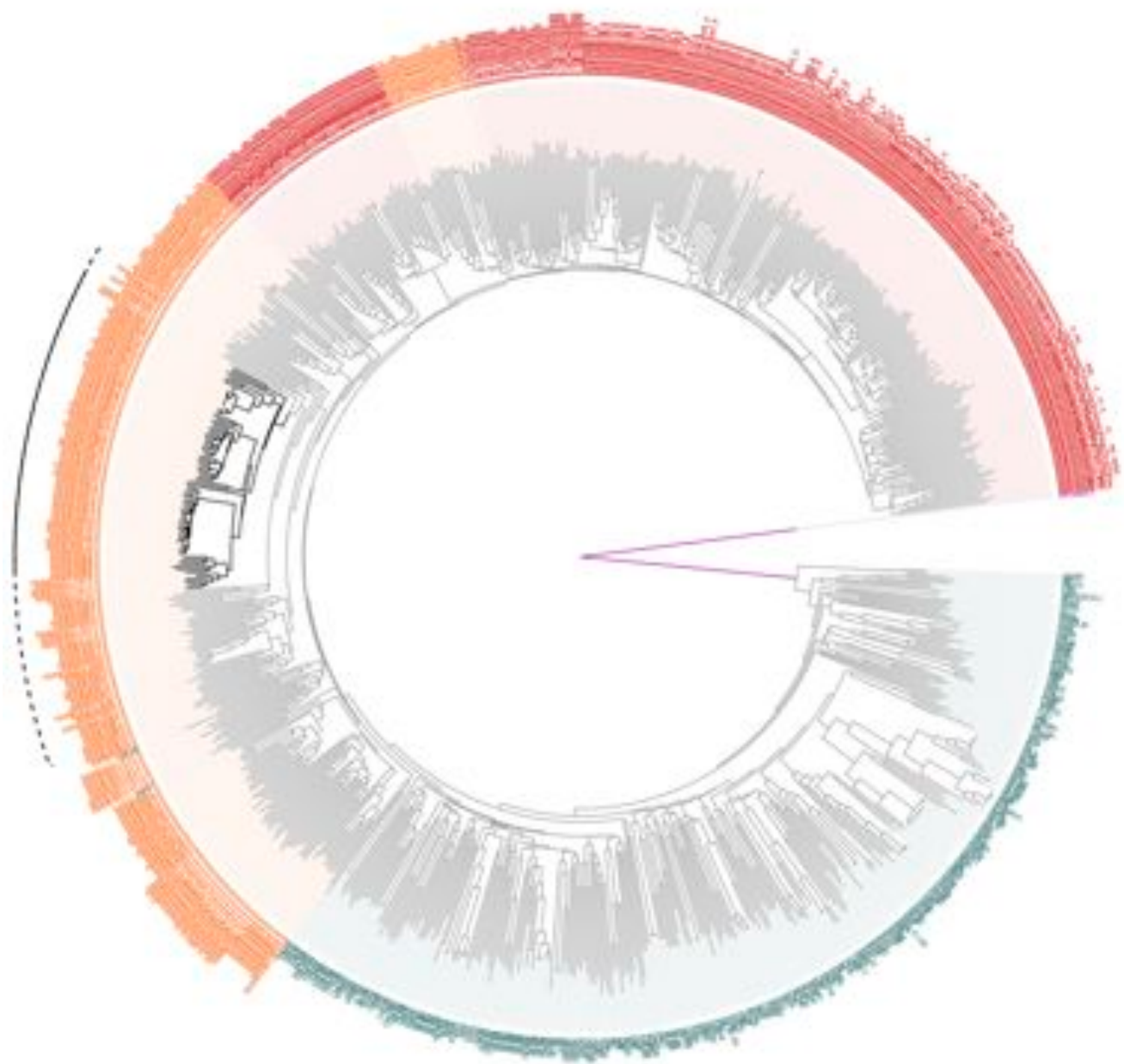


Figure S7

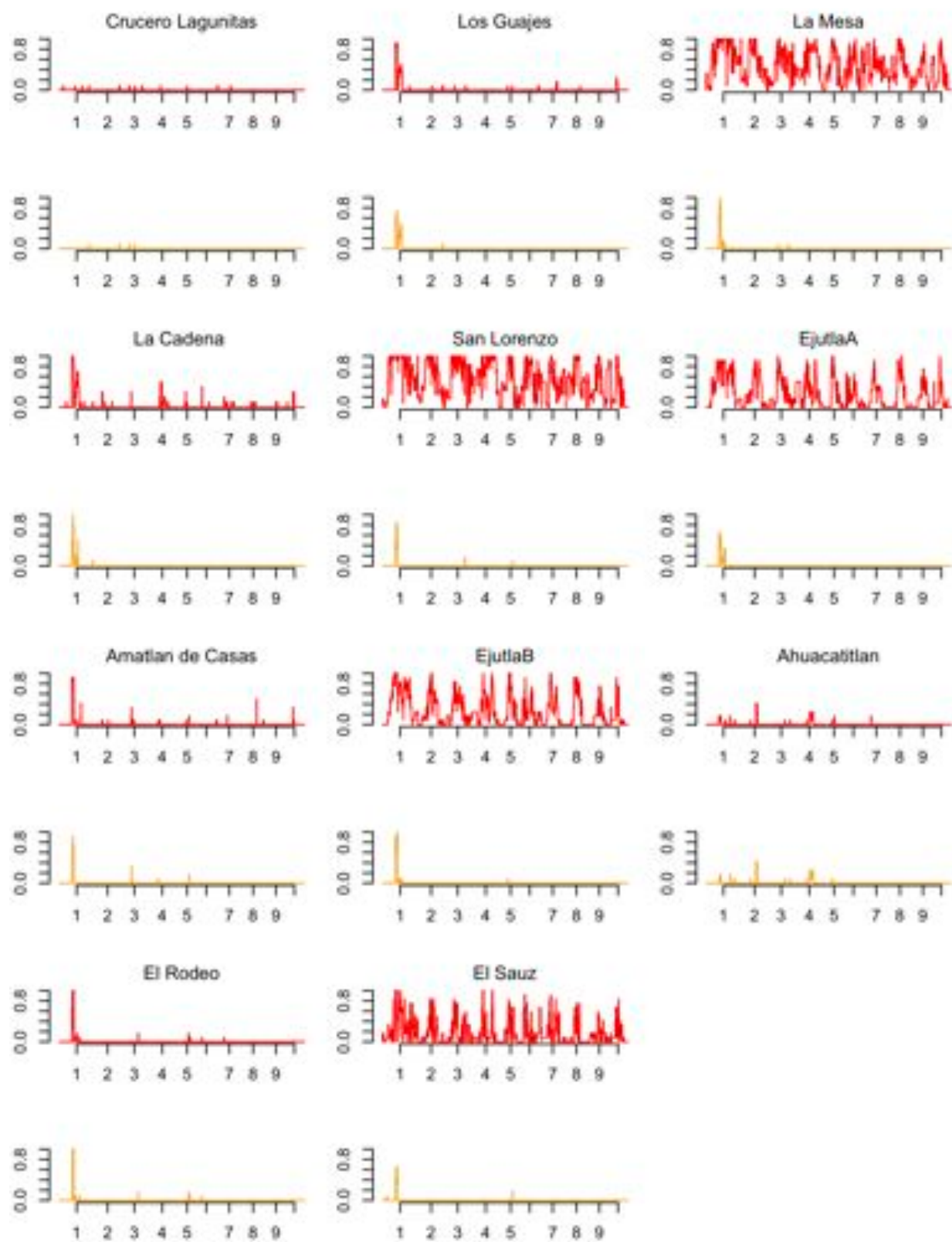


Figure S8

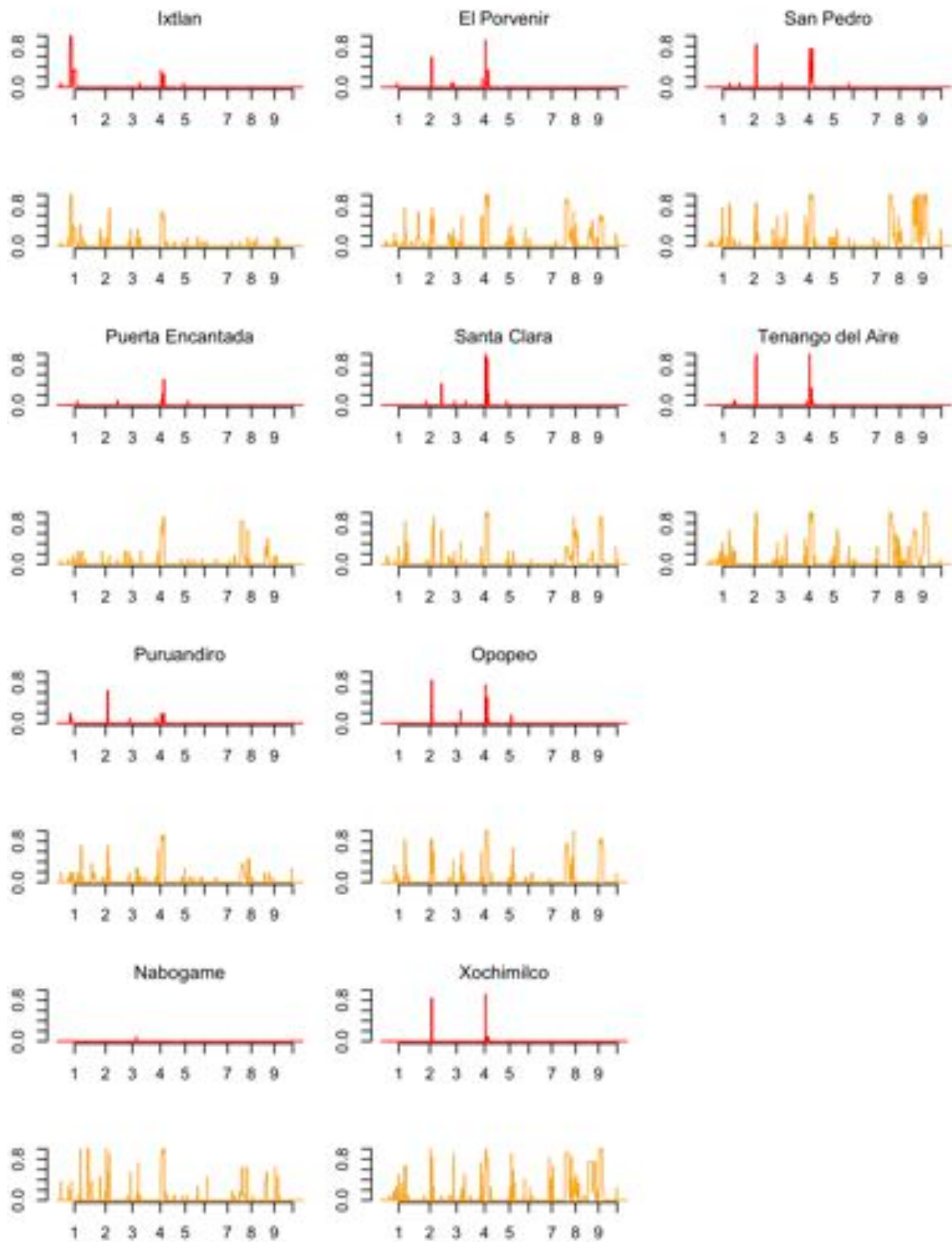


Figure S9

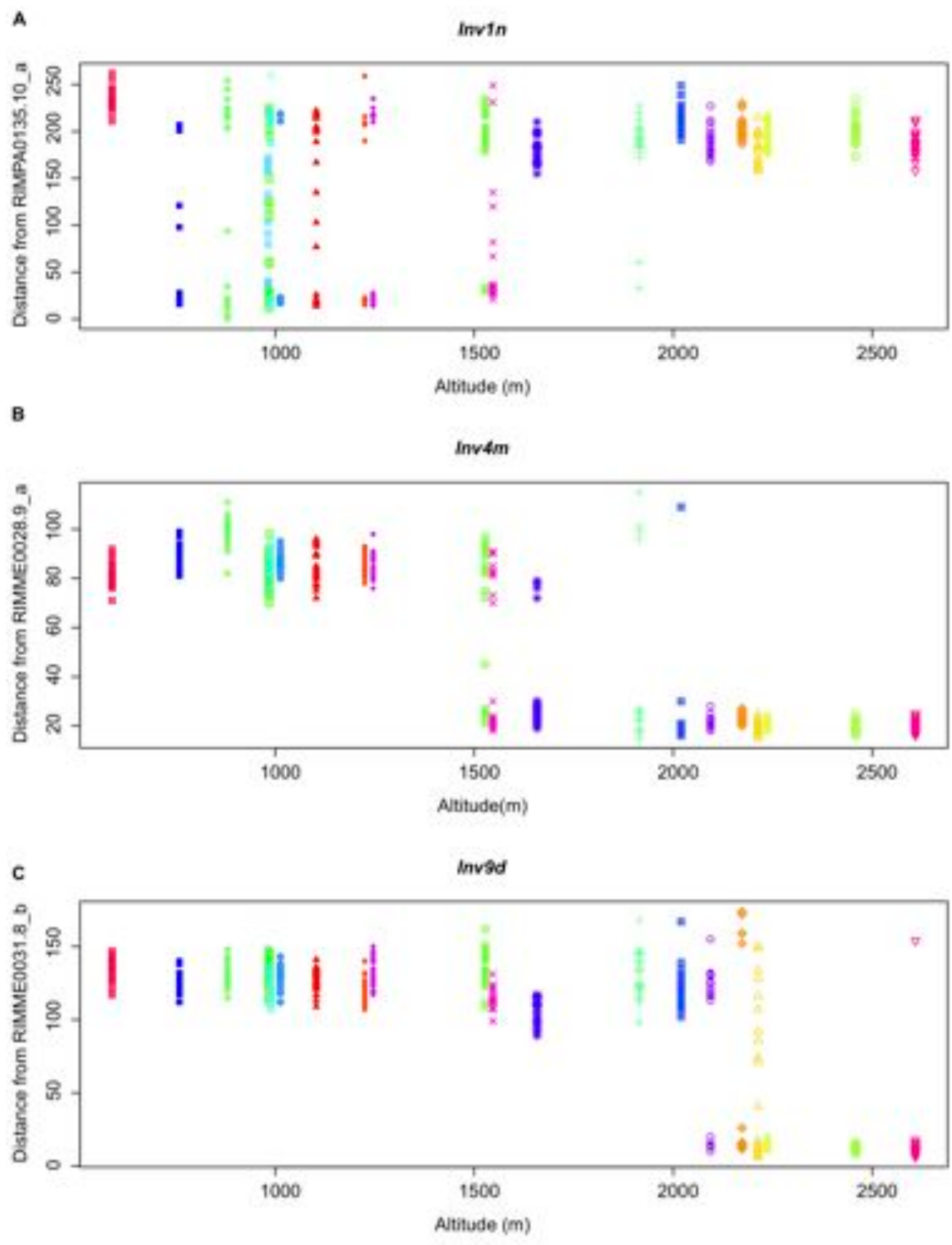


Figure S10

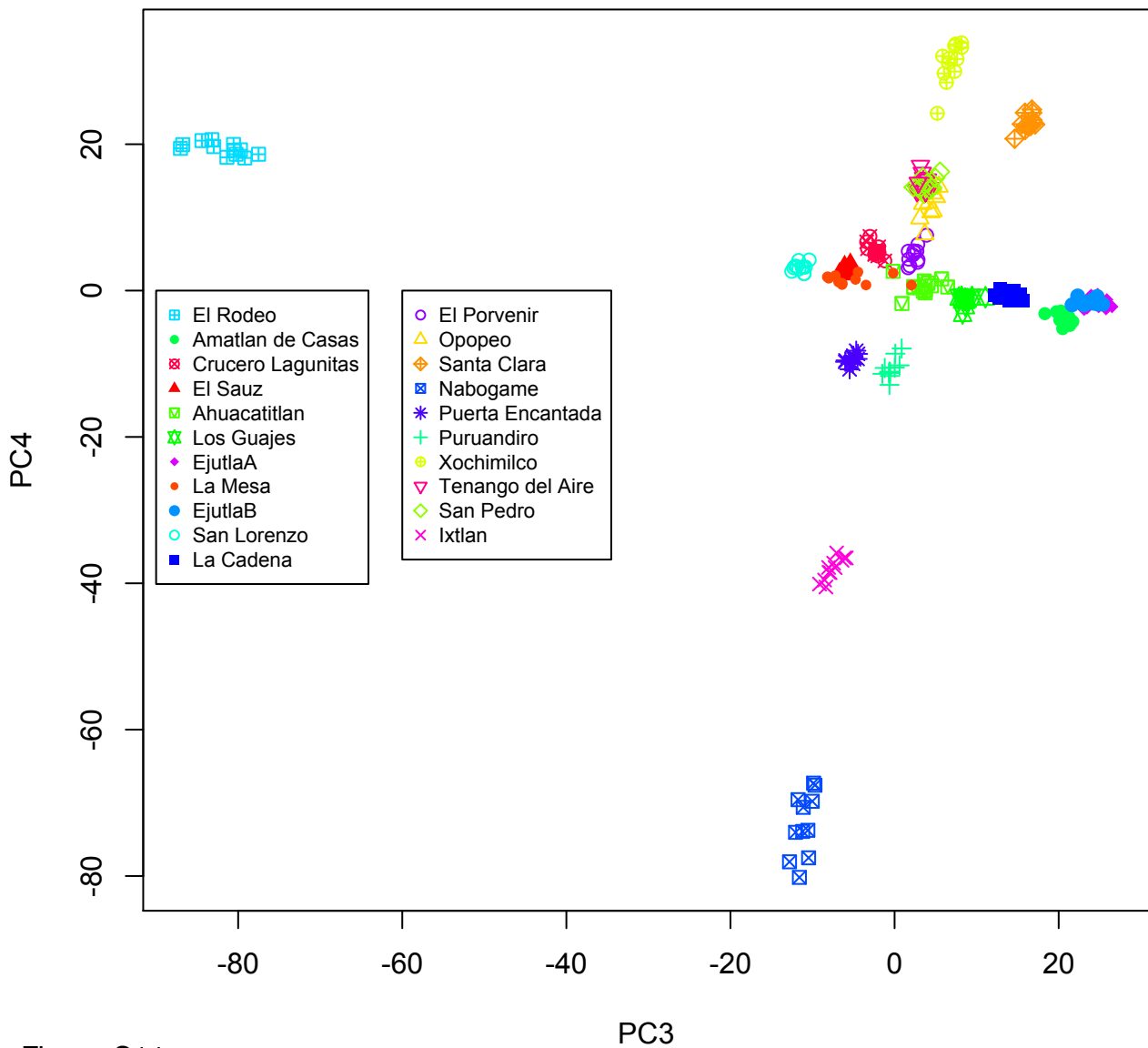
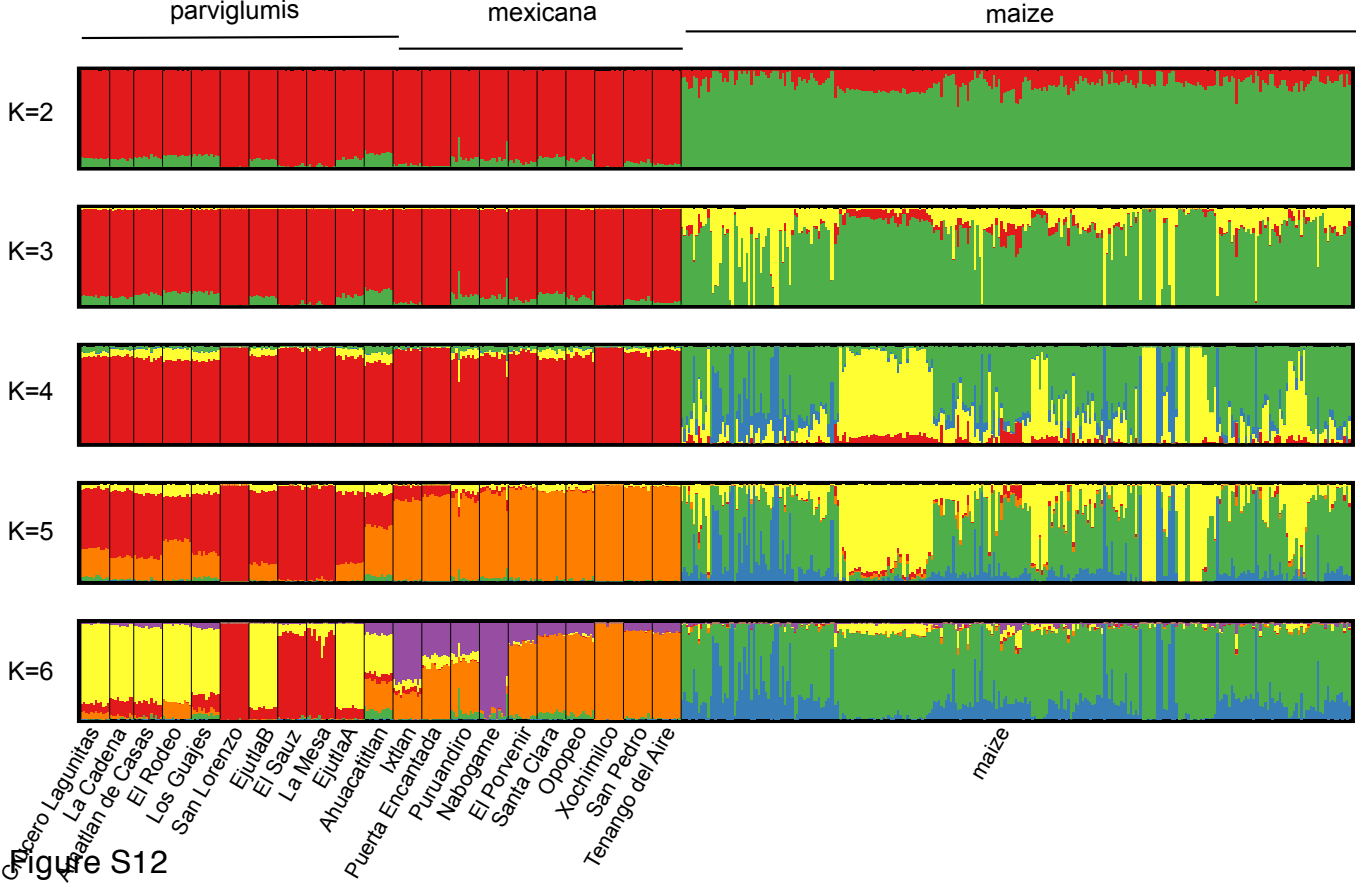


Figure S11





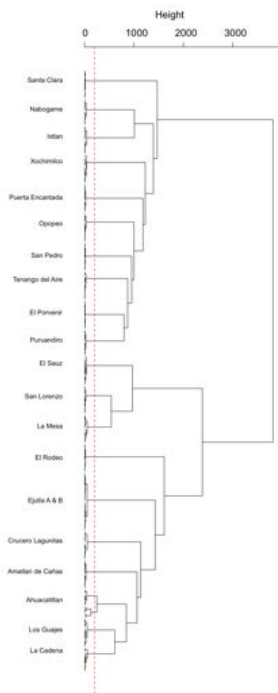


Figure S13

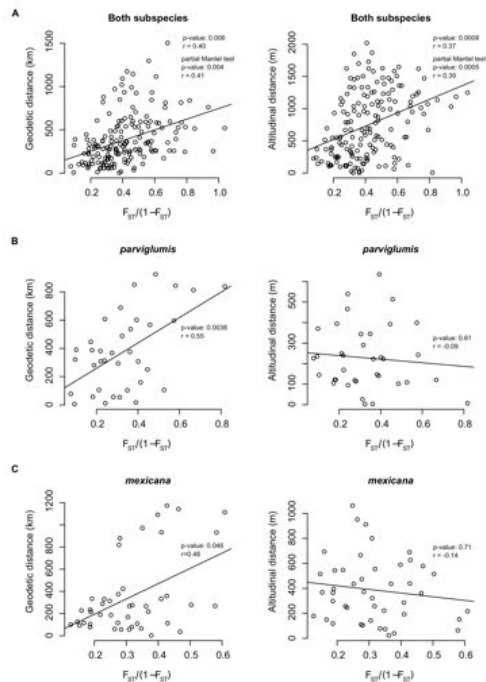
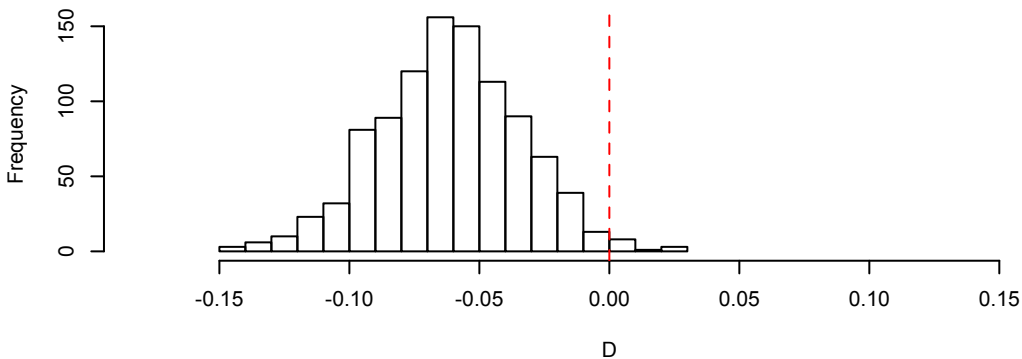
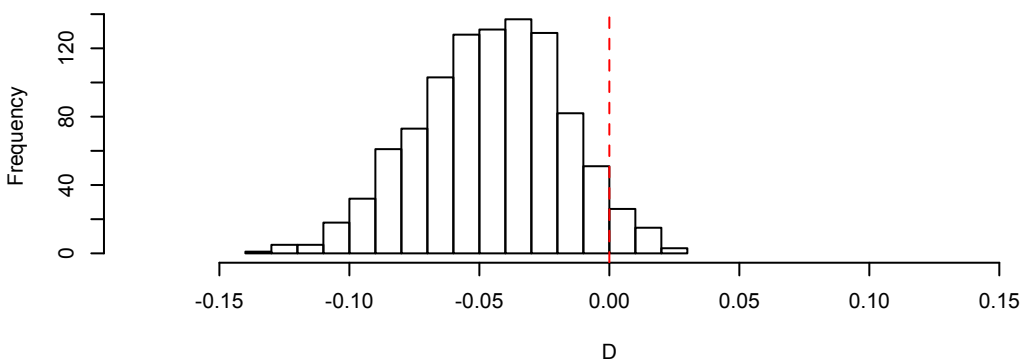


Figure S14

**Ahuacatitlan,(mexicana,parviglumis)**



**parviglumis,(mexicana,Ahuacatitlan)**



**mexicana,(parviglumis,Ahuacatitlan)**

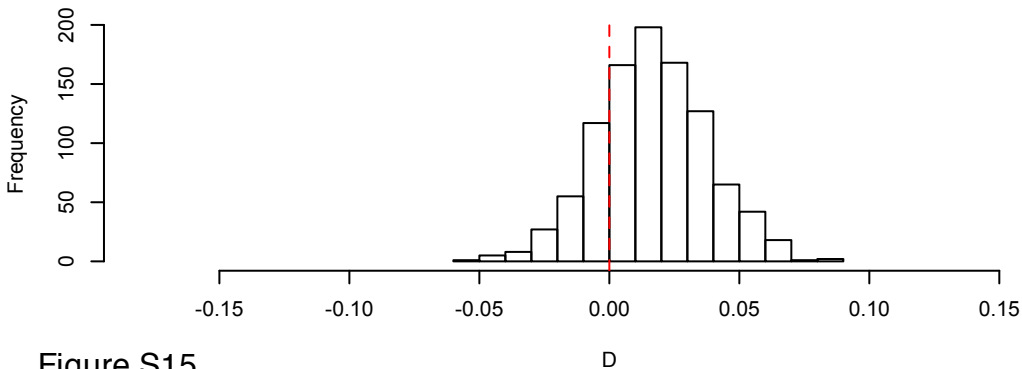


Figure S15

D

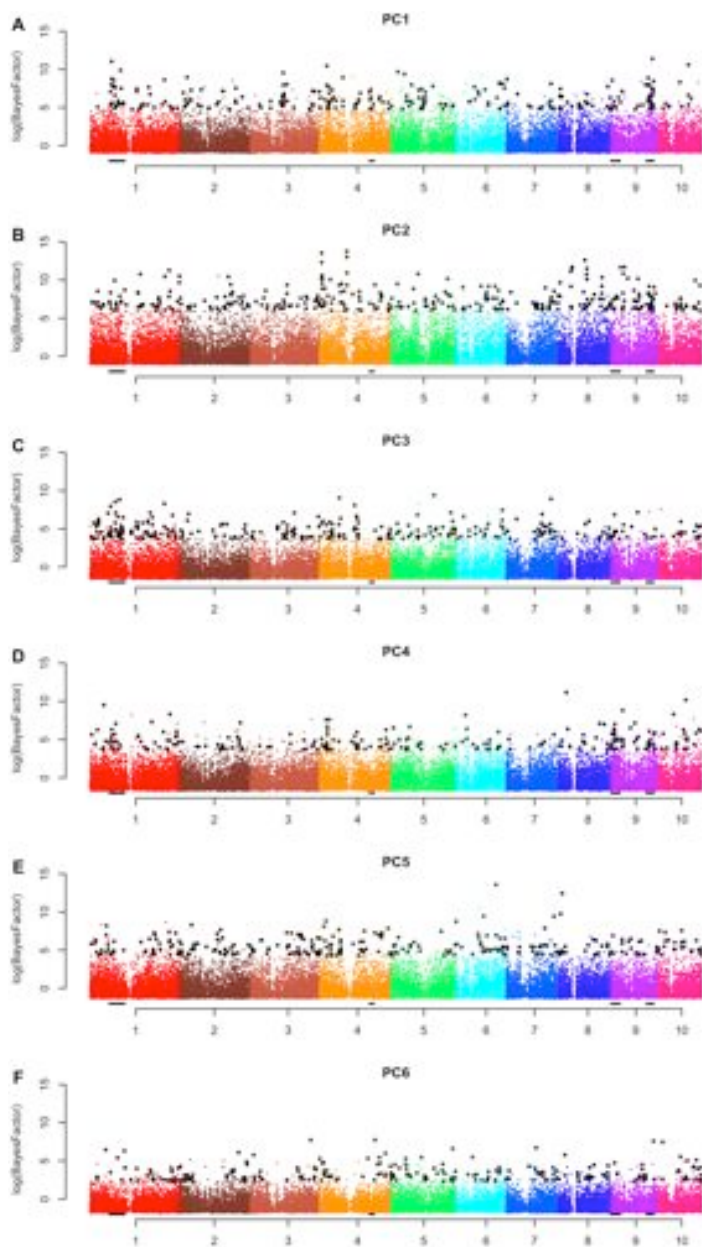


Figure S16

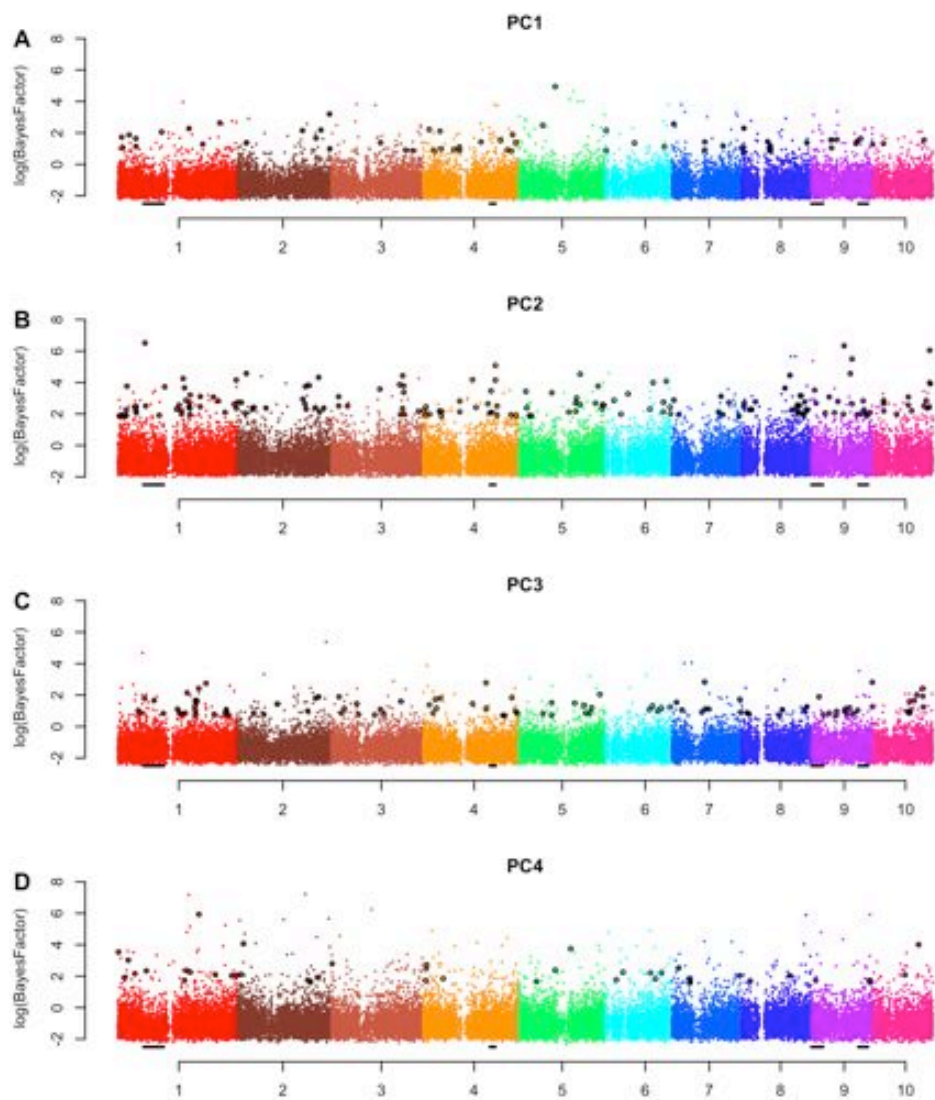


Figure S17

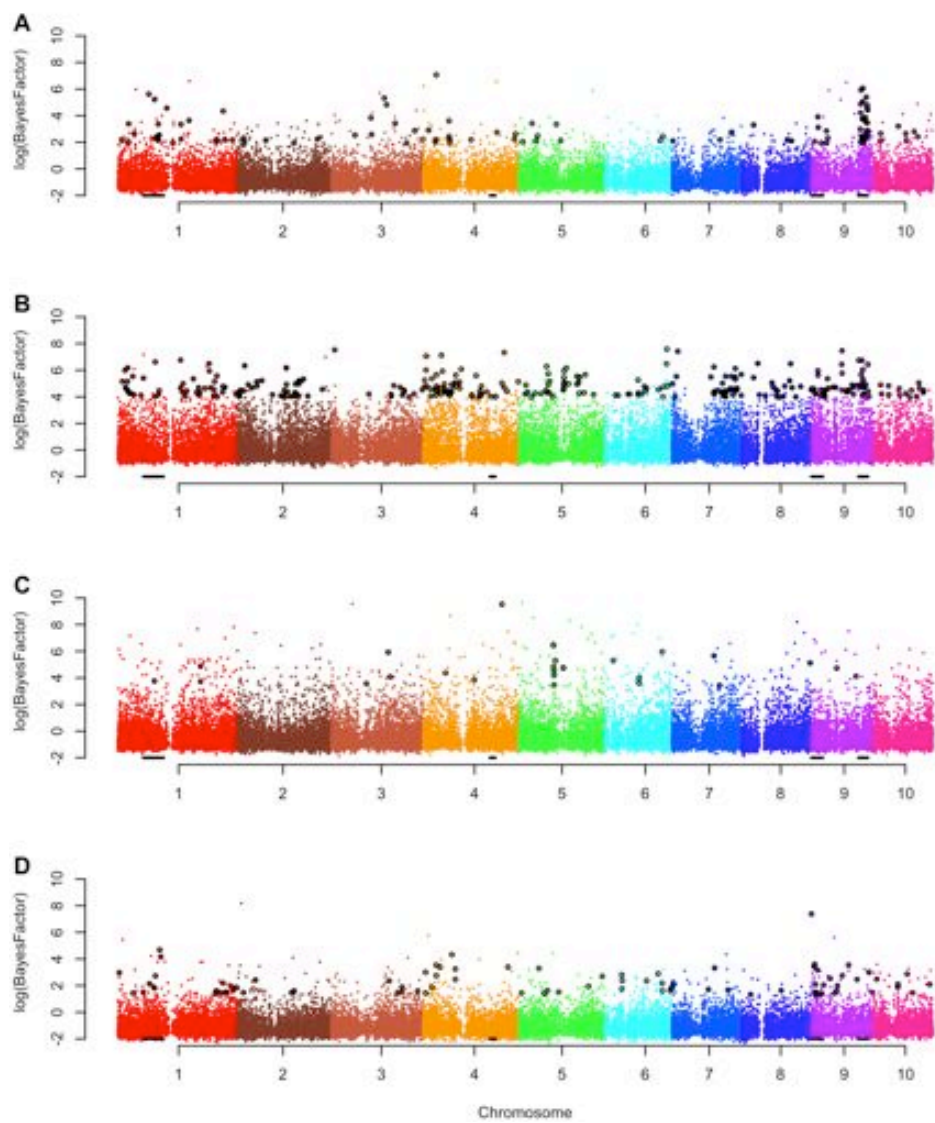


Figure S18

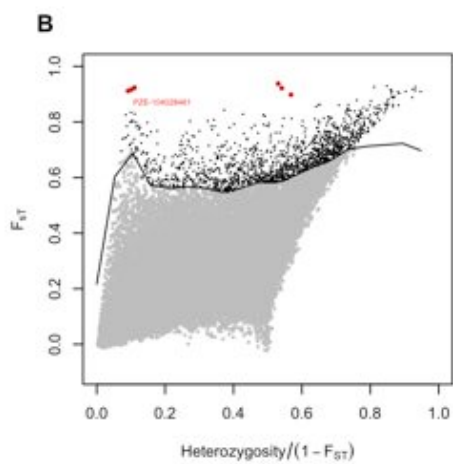
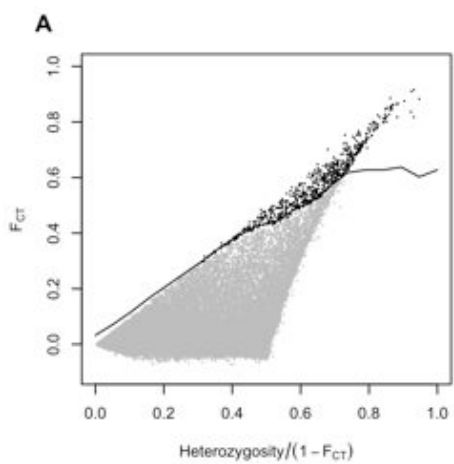


Figure S19



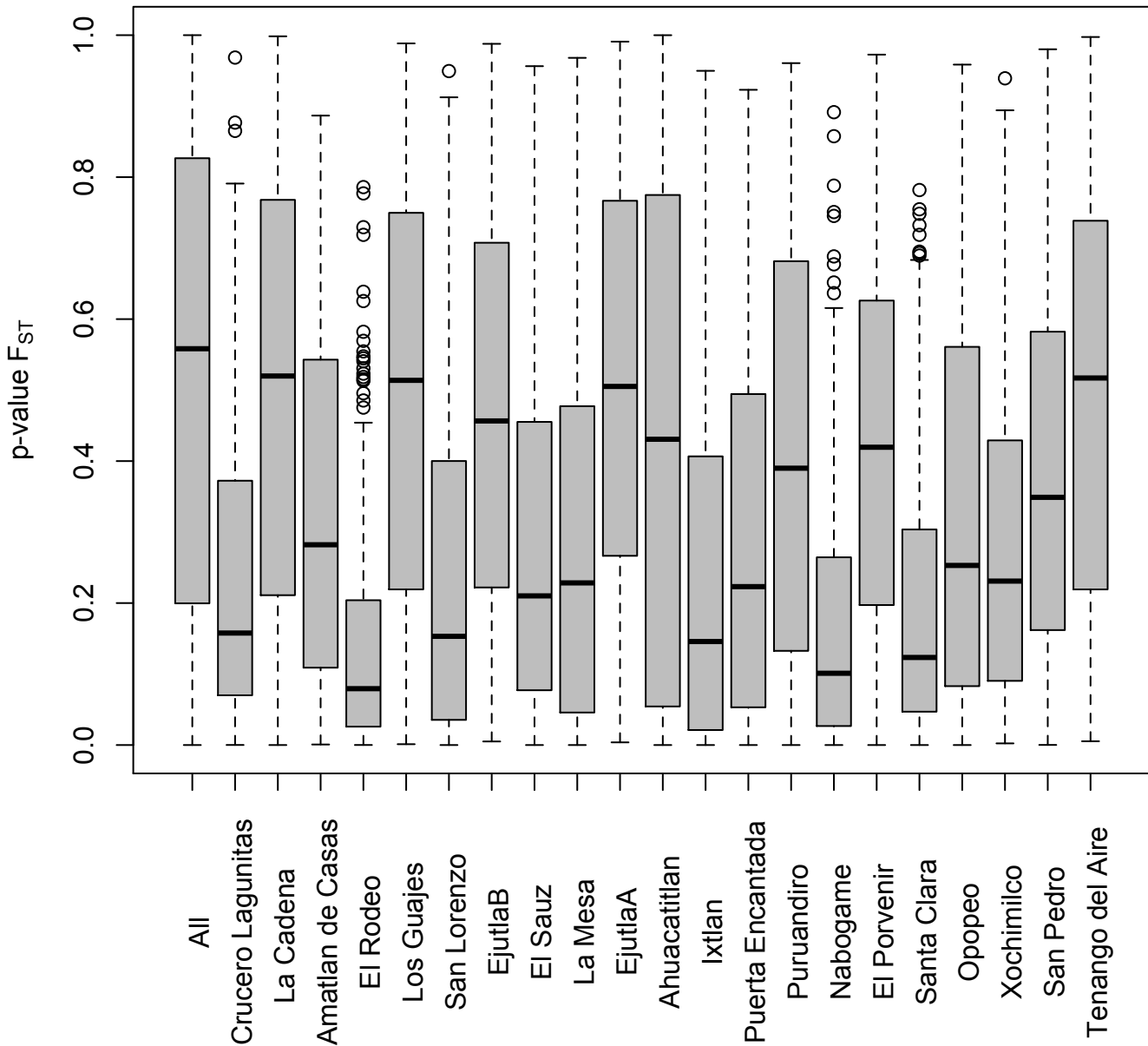


Figure S20

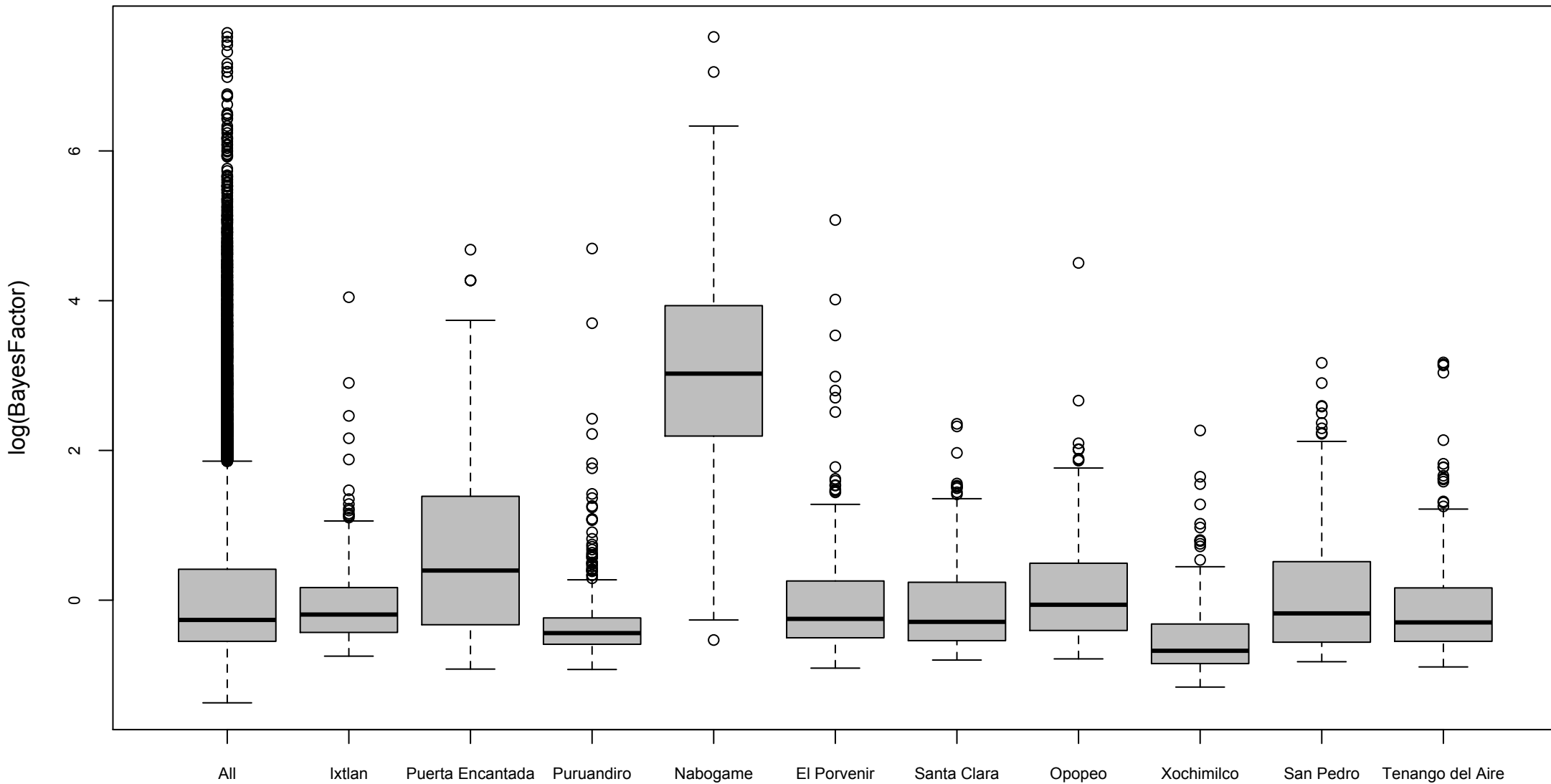


Figure 21

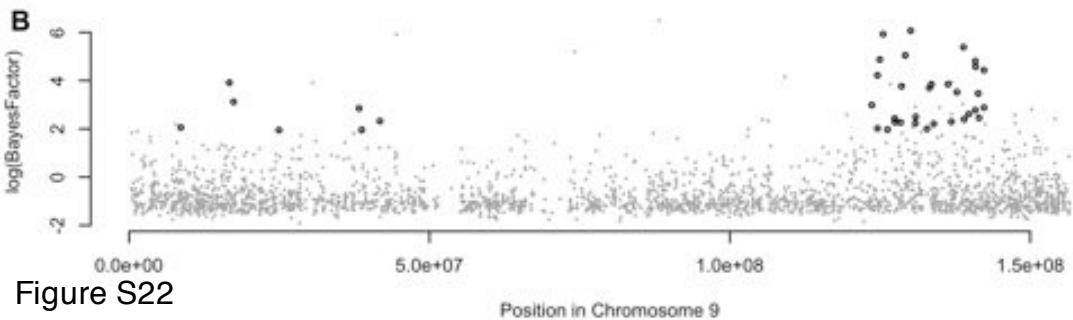
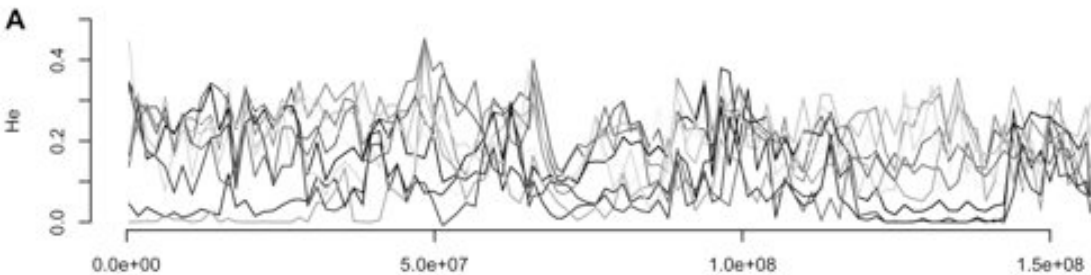


Figure S22



Figure S23

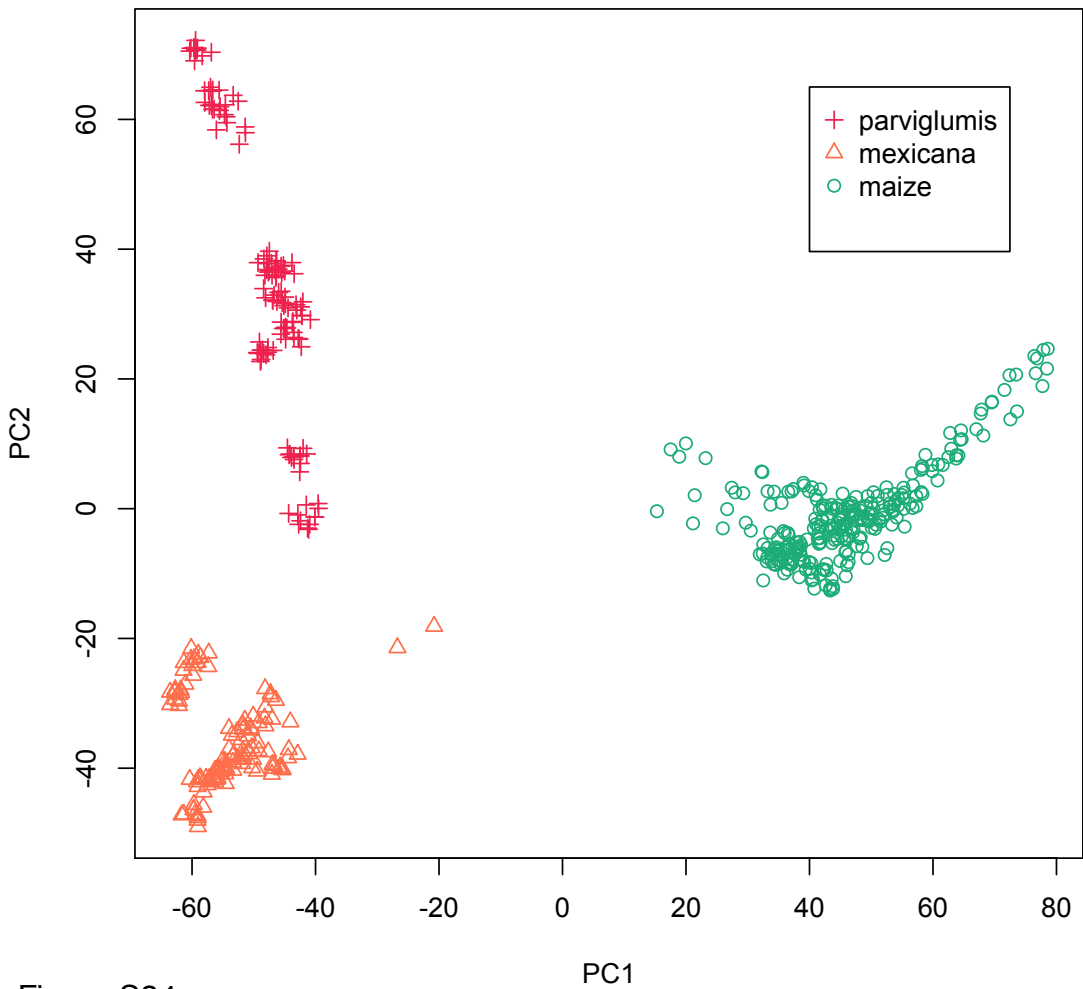


Figure S24

**Table S1** Summary statistics of genetic diversity for each population.

<b>Population</b>	<b>HWE</b>	<b>Polym.</b>	<b>H<sub>E</sub></b>	<b>F<sub>IS</sub></b>	<b>ROH length</b>	<b>IBS nr</b>	<b>IBS length</b>
Crucero Lagunitas	7%	62%	0.21	0.08	380	2.49	56
La Cadena	4%	72%	0.24	0.05	268	1.36	21
Amatlan de Casas	6%	64%	0.22	0.07	328	6.79	103
El Rodeo	6%	54%	0.18	0.03	282	6.70	103
Los Guajes	3%	80%	0.26	-0.01	71	0.70	10
San Lorenzo	5%	40%	0.13	-0.02	281	15.83	309
EjutlaB	4%	68%	0.23	0.02	206	4.22	54
El Sauz	6%	54%	0.17	0.03	333	9.39	156
La Mesa	5%	63%	0.19	0.01	204	9.52	134
EjutlaA	4%	71%	0.24	0.00	146	4.19	55
Ahuacatitlan	6%	75%	0.25	0.09	326	2.22	58
Ixtlan	7%	67%	0.20	0.08	339	1.84	29
Puerta Encantada	4%	52%	0.17	-0.01	209	6.15	114
Puruandiro	4%	75%	0.24	0.01	159	1.63	26
Nabogame	4%	62%	0.17	0.02	401	10.49	213
El Porvenir	4%	71%	0.22	0.02	174	2.49	37
Santa Clara	4%	56%	0.18	0.01	373	11.55	226
Opopeo	4%	69%	0.21	-0.01	207	5.99	103
Xochimilco	3%	44%	0.15	-0.02	773	11.19	498
San Pedro	3%	62%	0.20	-0.01	189	5.98	137
Tenango del Aire	4%	66%	0.20	0.02	227	3.80	74

HWE: proportion of SNPs deviating from HWE at 5% level, Polym.: proportion of polymorphic SNPs, H<sub>E</sub>: mean expected heterozygosity, F<sub>IS</sub>: mean inbreeding coefficient, ROH length: Average of total length of runs of homozygosity per individual (cM), IBS nr and length: Average of total number and length of identity-by-descent segments within population per individual, excluding comparisons within individuals (cM).

Table S2

Table S2 is available as an .xls file upon request from the authors.

**Table S3** Spearman's correlation between Bayes factors and p-values for  $F_{CT}$  and  $F_{ST}$ .

<b>Analysis</b>	<b>Variable</b>	<b><math>F_{CT}</math></b>		<b><math>F_{ST}</math></b>	
		<b>p-value</b>	<b>rho</b>	<b>p-value</b>	<b>rho</b>
Both	PC1	$3.8 \times 10^{-69}$	-0.09	$1.6 \times 10^{-292}$	-0.19
	PC2	0.03	-0.01	0	-0.20
	PC3	0.94	0.01	$6.2 \times 10^{-122}$	-0.12
	PC4	0.72	0.00	$1.3 \times 10^{-115}$	-0.12
	PC5	0.88	0.01	$3.1 \times 10^{-153}$	-0.14
	PC6	0.26	0.00	$3.6 \times 10^{-78}$	-0.10
<i>parviglumis</i>	PC1	$2.7 \times 10^{-23}$	-0.05	$1.1 \times 10^{-170}$	-0.15
	PC2	$5.5 \times 10^{-19}$	-0.05	$5.3 \times 10^{-167}$	-0.15
	PC3	$4.3 \times 10^{-23}$	-0.05	$9.7 \times 10^{-148}$	-0.14
	PC4	$9.4 \times 10^{-21}$	-0.05	$4.3 \times 10^{-132}$	-0.13
<i>mexicana</i>	PC1	$1.2 \times 10^{-02}$	-0.01	$1.1 \times 10^{-87}$	-0.11
	PC2	1.00	0.01	$3.2 \times 10^{-227}$	-0.17
	PC3	1.00	0.02	$6.6 \times 10^{-80}$	-0.10
	PC4	0.60	0.00	$1.9 \times 10^{-83}$	-0.10

p-values are for one-sided test where alternative hypothesis is that there is a negative correlation between p-values and Bayes factors. Rho is Spearman's rank correlation coefficient.



**Table S4** Enrichment of functional properties among candidate SNPs and genes.

<b>Analysis</b>	<b>p-value</b>	
	<b>gen/nongen</b>	<b>nonsyn/syn</b>
PC1	0.69	0.37
PC2	0.82	0.27
PC3	0.55	0.93
PC4	0.80	0.85
PC5	0.82	0.87
PC6	0.72	0.30
PC1 parv	0.90	0.20
PC2 parv	0.36	0.72
PC3 parv	0.54	0.60
PC4 parv	0.95	0.07
PC1 mex	0.87	0.04
PC2 mex	0.18	0.12
PC3 mex	0.92	0.17
PC4 mex	0.65	0.40
F <sub>CT</sub>	0.93	0.28
F <sub>ST</sub>	1.00	0.06

Analysis: candidate lists from different analyses, gen/nongen: p-value for observed ratio of genic and nongenic SNPs being higher than expected, nonsyn/syn: p-value for observed ratio of nonsynonymous and synonymous SNPs being higher than expected. All p-values are based on bootstrapping with 1000 iterations.

**Table S5** Enrichment of SNPs that are associated with a maize phenotypic trait for each list of adaptation candidates. GWAS was done using a mixed linear model that takes both population structure and relatedness into account.

<b>Trait</b>	<b>F<sub>CT</sub></b>	<b>F<sub>ST</sub></b>	<b>PC1</b>	<b>PC2</b>	<b>PC3</b>	<b>PC4</b>	<b>PC5</b>	<b>PC6</b>
20KernelWeight	0.636	0.169	0.661	0.085	0.160	0.689	0.760	0.190
CobDiameter	0.153	0.238	0.292	0.026	0.001	0.231	0.968	0.336
CobWeight	0.001	0.105	0.749	0.849	0.934	0.760	0.745	0.148
DaystoSilk	0.601	0.515	0.171	0.910	0.933	0.267	0.042	0.915
DaysToTassel	0.610	0.563	0.168	0.502	0.922	0.112	0.043	0.790
EarDiameter	0.365	0.320	0.427	0.393	0.004	0.494	0.260	0.685
EarLength	0.470	0.914	0.591	0.688	0.517	0.961	0.278	0.452
EarRankNumber	1.000	0.792	0.357	0.698	0.228	0.526	0.652	0.035
EarRowNumber	0.856	0.908	0.545	0.174	0.974	0.597	0.314	0.860
EarWeight	0.987	1.000	0.096	0.093	0.021	0.096	1.000	0.344
GerminationCount	0.009	0.019	0.709	0.044	0.208	0.372	0.689	0.464
LeafLength	0.582	0.531	0.023	0.440	0.393	0.521	0.076	0.587
LeafSheathLength	0.816	0.649	0.277	0.440	0.029	0.619	0.871	0.692
LeafWidth-BorderPlant	0.934	0.989	0.552	0.416	0.383	0.781	0.853	0.760
LeafWidth	0.292	0.763	0.186	0.986	0.881	0.388	0.093	0.664
MainSpikeLength	0.016	0.024	0.233	0.658	0.608	0.334	0.980	0.031
MiddleLeafAngle	0.326	0.150	0.171	0.413	0.602	0.378	0.414	0.934
NorthernLeafBlight	0.399	0.500	0.020	1.000	0.657	0.161	0.031	0.433
NumberofLeaves	0.517	0.902	0.190	0.712	0.136	0.158	0.288	0.131
NumberofTilleringPlants	0.346	0.283	0.031	0.893	0.680	0.095	0.210	0.153
Phylotaxy	0.958	0.845	0.816	0.391	0.305	0.680	0.417	0.008
RowQuality	0.029	0.383	0.115	0.478	0.722	0.270	0.250	0.277
SecondaryBranchNumber	0.723	0.993	0.389	0.551	0.257	0.138	0.922	0.141
SeedSetLength	0.827	0.142	0.933	0.840	0.329	0.857	0.636	0.730
Spikelets-MainSpike	0.392	0.298	0.292	0.936	0.322	0.439	0.840	0.054

Spikelets-PrimaryBranch	0.109	0.001	0.203	0.163	0.206	0.567	0.127	0.861
StandCount	0.021	0.000	0.367	0.009	0.620	0.017	0.291	0.218
TasselBranchLength	0.332	0.081	0.122	0.620	0.745	0.927	0.716	0.179
TasselLength	0.682	0.919	0.195	0.460	0.428	0.920	0.595	0.106
TasselPrimaryBranches	0.016	0.001	0.236	0.204	0.419	0.130	0.174	0.180
TasselSterility	0.334	0.427	0.639	0.003	0.094	0.536	0.069	0.775
TilleringIndex-BorderPlant	0.495	0.302	0.112	0.407	0.814	0.315	0.293	0.453
TilleringIndex	0.834	0.946	0.859	0.144	0.830	0.592	0.082	0.055
TotalKernelVolume	0.870	0.953	0.270	0.446	0.169	0.406	0.996	0.167
UpperLeafAngle-BorderPlant	0.985	0.854	0.980	0.002	0.160	0.346	0.552	0.488
UpperLeafAngle	0.401	0.190	0.750	0.787	0.949	0.484	0.224	0.193

Trait	PC1 parv	PC2 parv	PC3 parv	PC4 parv	PC1 mex	PC2 mex	PC3 mex	PC4 mex
20KernelWeight	0.015	0.262	0.288	1.000	0.540	0.964	0.004	0.765
CobDiameter	0.136	0.620	0.443	0.888	0.206	0.011	0.075	0.677
CobWeight	0.009	0.422	0.509	0.071	0.823	0.326	0.711	0.547
DaystoSilk	0.145	0.481	0.513	0.979	0.428	0.708	0.652	0.416
DaysToTassel	0.777	0.320	0.635	0.868	0.461	0.678	0.813	0.131
EarDiameter	0.002	0.891	0.140	0.293	0.032	0.563	0.901	0.394
EarLength	0.048	0.452	0.156	0.143	0.618	0.678	0.419	0.433
EarRankNumber	0.170	0.713	0.137	0.553	0.280	0.079	0.226	0.411
EarRowNumber	0.288	0.664	0.689	0.984	0.647	0.698	0.926	0.931
EarWeight	0.372	0.296	0.291	0.884	0.292	0.866	0.074	0.141
GerminationCount	0.058	0.112	0.608	0.719	0.978	0.793	0.713	0.116
LeafLength	0.000	0.028	0.407	0.804	0.165	0.622	0.100	0.787
LeafSheathLength	0.490	0.766	0.628	0.575	0.310	0.397	1.000	0.976
LeafWidth-BorderPlant	0.266	0.205	0.844	0.537	0.498	0.998	0.302	0.591
LeafWidth	0.154	0.159	0.367	0.049	0.121	0.987	0.554	0.936

MainSpikeLength	0.784	0.833	0.385	0.865	0.028	0.187	0.291	0.968
MiddleLeafAngle	0.170	0.158	0.769	0.751	0.761	0.463	0.086	0.402
NorthernLeafBlight	0.501	0.151	0.019	0.838	0.021	0.023	0.340	0.252
NumberOfLeaves	0.389	0.906	0.190	0.069	0.771	0.698	1.000	0.884
NumberOfTilleringPlants	0.905	0.538	0.905	0.793	0.142	0.504	0.666	0.522
Phylotaxy	0.945	0.257	0.123	0.528	0.525	0.498	0.691	0.984
RowQuality	0.612	0.629	0.514	0.291	0.211	0.145	0.677	0.818
SecondaryBranchNumber	0.355	0.243	0.397	0.094	0.645	0.390	0.859	0.303
SeedSetLength	0.634	0.580	0.298	0.065	0.782	0.705	0.008	0.487
Spikelets-MainSpike	0.233	0.510	0.462	0.460	0.495	0.637	0.897	0.097
Spikelets-PrimaryBranch	0.123	0.530	0.869	0.467	0.951	0.629	0.657	0.317
StandCount	0.382	0.421	0.426	0.389	0.673	0.072	0.056	0.259
TasselBranchLength	0.299	0.215	0.304	0.241	0.927	0.223	0.924	0.772
TasselLength	0.533	0.065	0.111	0.466	0.584	0.336	0.919	0.551
TasselPrimaryBranches	0.752	0.383	0.678	0.023	0.282	0.398	0.431	0.284
TasselSterility	0.780	0.751	0.906	1.000	0.120	0.229	0.498	0.894
TilleringIndex-BorderPlant	0.188	0.650	0.339	0.481	0.388	0.199	0.678	0.457
TilleringIndex	0.035	0.867	0.293	0.446	0.546	0.033	0.980	0.440
TotalKernelVolume	0.211	0.692	0.436	0.971	0.529	0.799	0.020	0.128
UpperLeafAngle-BorderPlant	0.767	0.659	0.851	0.833	0.113	0.171	1.000	0.253
UpperLeafAngle	0.795	0.044	0.779	0.984	0.911	0.962	0.925	0.416

**Table S6** Enrichment of SNPs that are associated with a maize phenotypic trait for each list of adaptation candidates. GWAS was done using a simple model not taking population structure into account.

<b>Trait</b>	<b>F<sub>CT</sub></b>	<b>F<sub>ST</sub></b>	<b>PC1</b>	<b>PC2</b>	<b>PC3</b>	<b>PC4</b>	<b>PC5</b>	<b>PC6</b>
20KernelWeight	0.780	0.215	0.852	0.650	0.913	0.526	0.217	0.629
CobDiameter	0.173	0.046	0.930	0.058	0.001	0.274	0.798	0.067
CobWeight	0.200	0.031	0.682	0.555	0.039	0.649	0.556	0.415
DaystoSilk	0.003	0.001	0.288	0.071	0.343	0.126	0.256	0.599
DaysToTassel	0.002	0.000	0.151	0.023	0.143	0.166	0.276	0.254
EarDiameter	0.216	0.003	0.339	0.082	0.233	0.130	0.971	0.676
EarLength	0.217	0.015	0.211	0.860	0.621	0.868	0.234	0.394
EarRankNumber	0.997	0.281	0.480	0.326	0.105	0.106	0.871	0.180
EarRowNumber	0.992	0.765	0.412	0.302	0.649	0.050	0.924	0.936
EarWeight	0.928	0.373	0.081	0.478	0.030	0.002	0.932	0.730
GerminationCount	0.888	0.968	0.448	0.618	0.155	0.110	0.785	0.204
LeafLength	0.000	0.002	0.397	0.205	0.063	0.275	0.376	0.542
LeafSheathLength	0.815	0.727	0.352	0.256	0.216	0.565	0.487	0.139
LeafWidth-BorderPlant	0.410	0.845	0.485	0.617	0.340	0.969	0.073	0.330
LeafWidth	0.019	0.005	0.286	0.728	0.306	0.585	0.162	0.489
MainSpikeLength	0.639	0.824	0.443	0.443	0.668	0.319	0.194	0.124
MiddleLeafAngle	0.209	0.001	0.620	0.446	0.068	0.414	0.039	0.916
NorthernLeafBlight	0.239	0.223	0.177	0.295	0.243	0.098	0.041	0.777
NumberofLeaves	0.110	0.095	0.082	0.702	0.054	0.411	0.464	0.487
NumberofTilleringPlants	0.008	0.004	0.005	0.900	0.190	0.156	0.059	0.216
Phylotaxy	0.981	0.894	0.600	0.955	0.180	0.810	0.133	0.190
RowQuality	0.035	0.473	0.021	0.001	0.899	0.045	0.047	0.247
SecondaryBranchNumber	0.080	0.050	0.147	0.407	0.122	0.048	0.714	0.020
SeedSetLength	0.047	0.328	0.940	0.985	0.467	0.931	0.392	0.861
Spikelets-MainSpike	0.005	0.025	0.401	0.023	0.161	0.280	0.486	0.349

Spikelets-PrimaryBranch	0.000	0.000	0.180	0.224	0.295	0.160	0.085	0.336
StandCount	0.202	0.000	0.462	0.369	0.496	0.287	0.441	0.155
TasselBranchLength	0.764	0.775	0.278	0.068	0.245	0.513	0.851	0.485
TasselLength	0.640	0.795	0.725	0.307	0.612	0.366	0.084	0.565
TasselPrimaryBranches	0.095	0.004	0.087	0.483	0.235	0.096	0.432	0.033
TasselSterility	0.144	0.057	0.486	0.241	0.209	0.987	0.108	0.594
TilleringIndex-BorderPlant	0.235	0.059	0.161	0.432	0.753	0.809	0.063	0.411
TilleringIndex	0.938	0.869	0.553	0.022	0.054	0.334	0.472	0.347
TotalKernelVolume	0.577	0.040	0.030	0.252	0.239	0.009	0.964	0.274
UpperLeafAngle-BorderPlant	0.854	0.272	0.964	0.124	0.274	0.005	0.290	0.345
UpperLeafAngle	0.297	0.000	0.220	0.031	0.689	0.007	0.643	0.810

<b>Trait</b>	<b>PC1 parv</b>	<b>PC2 parv</b>	<b>PC3 parv</b>	<b>PC4 parv</b>	<b>PC1 mex</b>	<b>PC2 mex</b>	<b>PC3 mex</b>	<b>PC4 mex</b>
20KernelWeight	0.256	0.762	0.463	0.998	0.718	0.484	0.279	0.405
CobDiameter	0.080	0.111	0.705	0.278	0.042	0.196	0.202	0.799
CobWeight	0.211	0.260	0.910	0.073	0.050	0.022	0.865	0.732
DaystoSilk	0.052	0.751	0.965	0.174	0.031	0.586	0.870	0.052
DaysToTassel	0.012	0.573	0.920	0.356	0.132	0.115	0.954	0.336
EarDiameter	0.124	0.947	0.971	0.099	0.011	0.001	0.565	0.993
EarLength	0.198	0.699	0.237	0.706	0.319	0.074	0.983	0.511
EarRankNumber	0.331	0.225	0.092	0.283	0.028	0.074	0.209	0.097
EarRowNumber	0.255	0.587	0.872	0.538	0.119	0.508	0.384	0.931
EarWeight	0.364	0.956	0.525	0.708	0.005	0.027	0.075	0.236
GerminationCount	0.022	0.415	0.444	0.342	0.856	0.556	0.643	0.186
LeafLength	0.058	0.085	0.923	0.087	0.789	0.334	0.889	0.643
LeafSheathLength	0.592	0.299	0.704	0.582	0.697	0.268	0.849	0.387
LeafWidth-BorderPlant	0.202	0.673	0.638	0.367	0.201	0.861	0.739	0.381
LeafWidth	0.016	0.685	0.551	0.149	0.304	0.726	0.668	0.250
MainSpikeLength	0.524	0.907	0.463	0.884	0.313	0.189	0.909	0.517

MiddleLeafAngle	0.014	0.356	0.171	0.635	0.473	0.207	0.650	0.040
NorthernLeafBlight	0.109	0.401	0.652	0.220	0.072	0.071	0.688	0.717
NumberOfLeaves	0.115	0.769	0.270	0.001	0.334	0.264	1.000	0.893
NumberOfTilleringPlants	0.340	0.167	0.883	0.878	0.167	0.458	0.389	0.301
Phylotaxy	0.930	0.333	0.037	0.557	0.705	0.505	0.704	0.919
RowQuality	0.154	0.721	0.543	0.760	0.087	0.002	0.774	0.726
SecondaryBranchNumber	0.488	0.718	0.785	0.222	0.360	0.423	0.652	0.355
SeedSetLength	0.743	0.618	0.279	0.101	0.493	0.853	0.106	0.368
Spikelets-MainSpike	0.018	0.302	0.761	0.408	0.308	0.502	0.687	0.385
Spikelets-PrimaryBranch	0.120	0.633	0.860	0.079	0.255	0.087	0.540	0.319
StandCount	0.765	0.095	0.744	0.664	0.775	0.029	0.619	0.308
TasselBranchLength	0.255	0.792	0.665	0.784	0.635	0.558	0.650	0.631
TasselLength	0.652	0.914	0.582	0.123	0.763	0.195	0.839	0.689
TasselPrimaryBranches	0.403	0.901	0.980	0.054	0.376	0.111	0.121	0.421
TasselSterility	0.306	0.826	0.848	1.000	0.318	0.157	1.000	0.821
TilleringIndex-BorderPlant	0.075	0.501	0.243	0.626	0.905	0.111	0.752	0.310
TilleringIndex	0.342	0.463	0.604	0.365	0.696	0.019	0.177	0.427
TotalKernelVolume	0.297	0.430	0.859	0.836	0.007	0.009	0.142	0.063
UpperLeafAngle-BorderPlant	0.528	0.055	0.082	0.559	0.035	0.416	0.080	0.282
UpperLeafAngle	0.608	0.526	0.203	0.364	0.104	0.261	0.536	0.188

**Table S7** Information about sampled populations ordered by ascending altitude.

<b>Population</b>	<b>Subspecies</b>	<b>N</b>	<b>Lat</b>	<b>Long</b>	<b>Alt</b>	<b>T</b>	<b>P</b>
Crucero Lagunitas	<i>parviglumis</i>	12	16.98	-99.28	590	26.2	1625
La Cadena	<i>parviglumis</i>	10	19.06	-101.21	759	26.6	1005
Amatlan de Casas	<i>parviglumis</i>	12	20.82	-104.41	880	24.4	849
El Rodeo	<i>parviglumis</i>	12	16.35	-97.02	982	22.3	1033
Los Guajes	<i>parviglumis</i>	12	19.23	-100.49	985	22.9	1049
San Lorenzo	<i>parviglumis</i>	12	19.95	-104.00	989	23.2	845
EjutlaB	<i>parviglumis</i>	12	19.91	-104.11	1013	23.2	891
El Sauz	<i>parviglumis</i>	12	19.44	-103.98	1103	22.4	1048
La Mesa	<i>parviglumis</i>	12	19.96	-104.05	1225	22.5	849
EjutlaA	<i>parviglumis</i>	12	19.90	-104.18	1246	21.3	809
Ahuacatitlan	<i>parviglumis</i>	12	18.36	-99.81	1528	22.3	1081
Ixtlan	<i>mexicana</i>	12	20.17	-102.37	1547	20.1	793
Puerta Encantada	<i>mexicana</i>	12	18.97	-99.03	1658	20.0	957
Puruandiro	<i>mexicana</i>	12	20.11	-101.49	1915	18.9	811
Nabogame	<i>mexicana</i>	12	26.25	-106.92	2020	15.8	978
El Porvenir	<i>mexicana</i>	12	19.68	-100.64	2094	16.4	918
Santa Clara	<i>mexicana</i>	12	19.42	-101.64	2173	15.5	1143
Opopeo	<i>mexicana</i>	12	19.42	-101.61	2213	15.6	1142
Xochimilco	<i>mexicana</i>	12	19.29	-99.08	2237	16.0	727
San Pedro	<i>mexicana</i>	12	19.09	-98.49	2459	14.3	1017
Tenango del Aire	<i>mexicana</i>	12	19.12	-99.59	2609	13.7	893

N: sample size, Lat: latitude, Long: longitude, Alt(m): altitude in meters above sea level, T: mean annual temperature in Celsius degrees, P: mean annual precipitation in millimeters



**Table S8** Environmental variables and abbreviations used in the study.

<b>Environmental variable</b>	<b>Abbreviation</b>
Annual Mean Temperature	bio1
Mean Diurnal Range (Mean of monthly (max temp - min temp))	bio2
Isothermality (bio2/bio7) (* 100)	bio3
Temperature Seasonality (standard deviation *100)	bio4
Max Temperature of Warmest Month	bio5
Min Temperature of Coldest Month	bio6
Temperature Annual Range (bio5-bio6)	bio7
Mean Temperature of Wettest Quarter	bio8
Mean Temperature of Driest Quarter	bio9
Mean Temperature of Warmest Quarter	bio10
Mean Temperature of Coldest Quarter	bio11
Annual Precipitation	bio12
Precipitation of Wettest Month	bio13
Precipitation of Driest Month	bio14
Precipitation Seasonality (Coefficient of Variation)	bio15
Precipitation of Wettest Quarter	bio16
Precipitation of Driest Quarter	bio17
Precipitation of Warmest Quarter	bio18
Precipitation of Coldest Quarter	bio19
Monthly mean, minimum and maximum temperature	tmean#, tmin#, tmax#
Monthly total precipitation	prec#
Rooting conditions <sup>1</sup>	sq3
Oxygen availability to roots <sup>2</sup>	sq4
Workability <sup>3</sup>	sq7
Sand in topsoil	ts_sand
Loam in topsoil	ts_loam
Clay in topsoil	ts_clay
Cracking clays	v_mod
Volcanic	

<sup>1</sup> Soil textures, bulk density, coarse fragments, vertical soil properties and soil phases affecting root penetration and soil depth and soil volume

<sup>2</sup> Soil drainage and soil phases affecting soil drainage

<sup>3</sup> Soil texture, effective soil depth/volume, and soil phases constraining soil management (soil depth, rock outcrop, stoniness, gravel/concretions and hardpans)

**Table S9** Variable loadings/rotations for each of 6 PCs that were used in BAYENV for the joint dataset of 20 *parviglumis* and *mexicana* populations

<b>PC1</b>		<b>PC2</b>		<b>PC3</b>		<b>PC4</b>		<b>PC5</b>		<b>PC6</b>	
<b>Var</b>	<b>Rot</b>	<b>Var</b>	<b>Rot</b>	<b>Var</b>	<b>Rot</b>	<b>Var</b>	<b>Rot</b>	<b>Var</b>	<b>Rot</b>	<b>Var</b>	<b>Rot</b>
bio1	0.146	bio4	0.244	prec7	0.287	ts_clay	0.410	bio2	0.380	bio2	0.412
tmean11	0.146	bio3	0.241	prec8	0.276	v_mod	0.359	sq4	0.328	x_mod	0.365
tmean12	0.145	bio7	0.241	prec11	0.262	ts_sand	0.329	ts_loam	0.289	sq7	0.332
bio11	0.145	prec6	0.237	bio13	0.247	bio15	0.272	ts_sand	0.266	bio7	0.312
tmax12	0.145	sq7	0.218	prec1	0.246	prec4	0.259	sq7	0.231	v_mod	0.307
tmin5	0.145	prec9	0.217	bio16	0.242	x_mod	0.244	bio18	0.213	prec11	0.230
tmean1	0.145	sq3	0.207	prec12	0.240	prec3	0.226	bio13	0.207	bio18	0.220
tmean2	0.145	prec12	0.207	bio19	0.238	sq3	0.210	prec11	0.183	sq3	0.176
tmin4	0.145	bio12	0.204	bio12	0.231	prec5	0.210	bio7	0.170	sq4	0.153
tmax1	0.145	bio19	0.196	prec2	0.222	prec7	0.190	bio16	0.163	ts_sand	0.153
tmean4	0.145	prec2	0.188	bio18	0.221	sq4	0.186	bio4	0.157	bio4	0.148
tmin11	0.144	prec1	0.185	sq4	0.200	bio3	0.185	bio12	0.156	prec7	0.139
tmax11	0.144	prec10	0.184	prec9	0.180	bio18	0.178	bio3	0.155	tmax3	0.127
tmin12	0.144	bio16	0.183	prec10	0.171	sq7	0.132	prec6	0.154	tmax4	0.126
tmin2	0.144	prec8	0.170	prec5	0.161	bio14	0.116	x_mod	0.152	bio5	0.118
tmean5	0.144	prec5	0.165	prec4	0.154	bio13	0.099	prec9	0.144	tmax5	0.115
tmean10	0.144	bio14	0.158	sq3	0.147	bio16	0.095	prec8	0.143	bio3	0.107
bio6	0.144	bio13	0.151	bio2	0.143	prec8	0.090	v_mod	0.142	ts_loam	0.095
tmax2	0.144	bio17	0.149	bio17	0.129	bio7	0.077	bio15	0.136	ts_clay	0.078
tmean3	0.144	prec3	0.144	ts_loam	0.127	bio4	0.075	prec7	0.112	tmin9	0.072
tmin1	0.143	ts_clay	0.141	v_mod	0.123	bio2	0.074	prec4	0.108	tmin8	0.071
tmin10	0.143	bio2	0.129	prec3	0.113	prec2	0.074	bio14	0.096	prec9	0.070
Altitude	0.143	prec7	0.108	x_mod	0.111	bio19	0.068	tmax7	0.093	tmin10	0.069
bio9	0.143	tmax6	0.107	bio14	0.099	prec12	0.056	tmax8	0.092	tmin12	0.069
tmin3	0.143	x_mod	0.106	bio4	0.070	ts_loam	0.053	prec1	0.091	tmin7	0.066
bio10	0.142	bio15	0.098	tmax3	0.067	tmax12	0.047	prec2	0.086	tmean4	0.066
tmax10	0.142	ts_loam	0.088	ts_clay	0.065	bio17	0.047	tmin11	0.086	tmax2	0.066
tmax3	0.142	tmean6	0.085	bio15	0.056	bio9	0.043	prec5	0.082	tmax6	0.064
tmax4	0.142	tmin7	0.082	tmax2	0.055	tmax8	0.042	bio17	0.082	tmean3	0.064

tmin6	0.142	bio5	0.082	tmean3	0.052	tmax1	0.041	tmin12	0.080	bio9	0.058
tmean9	0.141	tmean7	0.081	ts_sand	0.050	tmax5	0.039	prec3	0.078	tmin11	0.058
tmin9	0.141	prec4	0.080	prec6	0.048	tmax7	0.039	tmax9	0.078	prec3	0.056
tmean8	0.141	tmax7	0.079	sq7	0.048	prec10	0.038	tmin1	0.077	tmean5	0.056
bio8	0.140	bio8	0.079	tmin7	0.046	Altitude	0.037	tmin10	0.074	bio10	0.051
tmean6	0.140	tmax9	0.077	bio3	0.044	tmax10	0.035	bio6	0.071	bio15	0.047
tmean7	0.140	tmean8	0.076	tmax4	0.043	tmax2	0.033	prec12	0.067	tmin1	0.045
tmin8	0.140	tmin8	0.076	bio7	0.042	tmax9	0.030	tmin2	0.061	prec12	0.045
tmax5	0.140	tmax5	0.074	tmax1	0.036	tmean12	0.029	tmin6	0.061	bio17	0.045
tmax9	0.139	tmax8	0.074	tmin3	0.035	tmax11	0.027	tmax6	0.059	tmean10	0.043
tmax8	0.139	tmean9	0.072	bio9	0.035	tmean1	0.027	tmin3	0.052	prec4	0.043
bio5	0.139	bio18	0.070	tmin8	0.034	bio5	0.026	bio8	0.046	Altitude	0.041
tmax7	0.139	v_mod	0.066	tmean4	0.031	tmean5	0.026	tmean11	0.041	bio6	0.039
tmin7	0.138	tmin9	0.066	tmean2	0.031	bio11	0.025	tmean1	0.040	tmin6	0.038
tmax6	0.135	bio10	0.065	tmax12	0.030	tmean2	0.022	tmin9	0.040	tmean12	0.035
bio17	0.107	tmax10	0.063	tmean7	0.028	tmin6	0.022	tmean12	0.040	tmean9	0.035
bio14	0.095	tmin6	0.061	tmin9	0.023	prec1	0.022	tmax10	0.038	prec5	0.033
prec3	0.094	prec11	0.056	Altitude	0.021	tmean7	0.020	tmin5	0.038	tmean8	0.030
bio15	0.092	ts_sand	0.054	tmax11	0.019	tmean8	0.020	bio11	0.037	tmin2	0.030
prec4	0.088	sq4	0.049	tmin4	0.018	tmean9	0.019	tmean8	0.035	tmax1	0.030
prec10	0.084	tmin3	0.048	tmax5	0.017	prec11	0.019	tmean7	0.033	prec1	0.025
ts_sand	0.073	tmean10	0.047	tmin10	0.017	tmean11	0.018	tmean2	0.030	bio13	0.024
ts_loam	0.072	tmean5	0.044	tmin6	0.017	tmax4	0.016	bio19	0.029	tmean11	0.023
prec6	0.069	tmax4	0.042	tmean6	0.017	tmean10	0.016	bio9	0.027	tmax7	0.023
prec9	0.063	tmax11	0.041	tmax6	0.017	tmin5	0.015	tmin7	0.026	tmean7	0.023
prec2	0.063	bio6	0.038	tmin12	0.017	tmean6	0.015	tmin4	0.025	prec10	0.022
bio4	0.060	tmin1	0.038	bio11	0.016	prec6	0.014	tmean5	0.023	prec2	0.020
prec5	0.058	tmin2	0.037	tmin11	0.015	bio6	0.012	tmean3	0.022	bio8	0.018
bio13	0.055	Altitude	0.036	tmin1	0.013	tmin1	0.012	tmin8	0.022	tmean2	0.017
x_mod	0.053	tmin10	0.034	tmean5	0.013	tmin12	0.011	tmean10	0.021	bio16	0.016
prec1	0.050	bio9	0.032	tmean8	0.013	tmin2	0.011	tmean9	0.019	tmean6	0.014
bio16	0.049	tmean1	0.029	bio6	0.012	bio1	0.011	tmean4	0.019	bio19	0.012
bio7	0.043	bio1	0.028	tmean9	0.010	tmin4	0.009	ts_clay	0.018	tmax11	0.012

bio19	0.042	tmean3	0.026	tmean1	0.010	tmax6	0.008	prec10	0.015	tmax10	0.011
bio12	0.042	tmean2	0.024	bio10	0.010	tmin11	0.007	bio1	0.014	tmax8	0.010
bio3	0.040	bio11	0.022	tmax8	0.009	bio8	0.007	tmax4	0.014	tmean1	0.009
prec7	0.034	tmean11	0.019	tmax7	0.009	bio10	0.007	bio10	0.011	bio14	0.009
prec12	0.033	tmin12	0.019	bio5	0.008	tmin9	0.006	tmax5	0.009	prec8	0.007
bio2	0.033	tmax1	0.017	tmin5	0.008	prec9	0.005	bio5	0.008	bio11	0.007
prec8	0.032	tmean4	0.016	tmin2	0.007	bio12	0.004	tmax11	0.008	tmin5	0.006
sq4	0.026	tmin5	0.013	bio1	0.007	tmax3	0.003	tmax12	0.008	tmax9	0.005
sq3	0.024	tmean12	0.012	tmax10	0.006	tmean4	0.003	tmax3	0.007	bio12	0.004
v_mod	0.015	tmax2	0.011	tmean10	0.006	tmin3	0.002	sq3	0.007	tmin3	0.004
ts_clay	0.012	tmin4	0.010	tmean12	0.005	tmin7	0.002	tmax2	0.006	prec6	0.004
sq7	0.004	tmax3	0.003	bio8	0.004	tmean3	0.002	Altitude	0.004	tmin4	0.003
prec11	0.004	tmax12	0.002	tmax9	0.003	tmin10	0.002	tmean6	0.002	bio1	0.002
bio18	0.001	tmin11	0.001	tmean11	0.001	tmin8	0.000	tmax1	0.001	tmax12	0.002

**Table S10** Variable loadings/rotations for each of 4 PCs that were used in BAYENV for 10 *parviglumis* populations

<b>PC1</b>		<b>PC2</b>		<b>PC3</b>		<b>PC4</b>	
<b>Var</b>	<b>Rot</b>	<b>Var</b>	<b>Rot</b>	<b>Var</b>	<b>Rot</b>	<b>Var</b>	<b>Rot</b>
tmax12	0.145	bio4	0.258	x_mod	0.300	prec4	0.315
bio1	0.144	bio7	0.248	ts_loam	0.300	prec11	0.278
bio11	0.144	bio3	0.232	prec5	0.241	prec1	0.276
tmean2	0.143	ts_clay	0.205	prec11	0.214	bio2	0.256
tmean12	0.143	prec9	0.185	ts_sand	0.214	prec5	0.233
tmax1	0.143	bio12	0.185	prec4	0.196	prec12	0.222
tmean11	0.142	prec10	0.184	bio15	0.194	ts_clay	0.213
tmean1	0.142	tmax6	0.177	bio2	0.186	bio19	0.208
tmin5	0.142	prec6	0.173	bio18	0.176	x_mod	0.183
tmean3	0.141	tmax5	0.169	prec8	0.165	ts_loam	0.183
tmax2	0.140	bio2	0.167	prec12	0.161	tmax8	0.170
tmin4	0.139	bio5	0.165	prec7	0.159	sq3	0.166
Altitude	0.139	tmean6	0.160	tmin10	0.157	sq7	0.166
bio9	0.139	prec8	0.157	sq3	0.155	bio18	0.164
tmax11	0.138	bio16	0.157	sq7	0.155	tmax9	0.149
tmin2	0.138	ts_sand	0.156	bio13	0.151	tmin12	0.131
tmin3	0.138	prec5	0.155	tmax3	0.146	tmax7	0.130
tmean4	0.137	bio13	0.139	tmin7	0.145	tmin11	0.125
tmin11	0.136	prec1	0.138	tmin9	0.142	bio17	0.124
bio6	0.135	bio17	0.136	tmin8	0.142	bio9	0.119
bio10	0.134	tmin6	0.127	bio16	0.141	bio3	0.118
tmean5	0.133	tmin7	0.126	bio7	0.129	prec2	0.116
tmax3	0.133	tmax4	0.125	prec2	0.129	tmin1	0.113
tmin1	0.133	tmin9	0.120	tmax4	0.128	tmean8	0.111
tmin12	0.132	bio8	0.120	tmax2	0.115	bio8	0.108
tmean10	0.130	tmean7	0.119	prec9	0.112	tmean9	0.106
tmax10	0.128	tmean9	0.117	tmean4	0.111	prec10	0.106
tmax7	0.128	tmin8	0.116	tmean10	0.110	tmax10	0.102
tmean7	0.127	bio14	0.116	tmean3	0.106	bio6	0.102
tmean8	0.126	tmax9	0.113	bio5	0.096	bio7	0.096

tmin10	0.125	tmax10	0.112	tmin12	0.090	tmin2	0.088
bio8	0.125	tmean8	0.110	tmin11	0.088	prec7	0.082
tmax8	0.125	prec4	0.110	tmax5	0.085	Altitude	0.081
tmin6	0.125	bio10	0.109	tmean9	0.085	tmean7	0.073
tmean9	0.125	tmax7	0.107	tmean7	0.083	tmin4	0.071
tmax9	0.123	prec2	0.105	tmean5	0.082	bio4	0.070
tmax4	0.122	tmean10	0.098	bio12	0.080	tmin3	0.068
tmin8	0.121	tmean5	0.096	tmin4	0.079	tmin6	0.068
tmean6	0.120	tmax8	0.096	prec1	0.079	ts_sand	0.066
tmin9	0.119	prec12	0.095	tmean8	0.078	tmean12	0.063
bio19	0.118	tmax11	0.094	tmin6	0.077	tmin5	0.058
tmin7	0.118	tmin1	0.086	prec10	0.069	prec3	0.055
prec7	0.117	tmin10	0.081	tmax1	0.068	tmean11	0.053
prec2	0.117	bio6	0.080	tmean2	0.066	tmax6	0.050
prec3	0.116	bio18	0.077	tmin5	0.066	prec6	0.049
bio13	0.113	prec3	0.072	bio3	0.062	bio11	0.049
bio5	0.113	prec7	0.071	bio8	0.058	tmean4	0.048
tmax6	0.112	tmin2	0.070	tmin3	0.057	tmean5	0.046
tmax5	0.112	sq7	0.069	tmax10	0.055	tmin9	0.045
sq3	0.112	sq3	0.069	tmax12	0.053	tmean10	0.042
sq7	0.112	tmin3	0.068	bio17	0.050	tmean1	0.041
bio17	0.108	bio19	0.067	bio9	0.049	tmax2	0.039
prec6	0.108	tmean1	0.062	bio10	0.047	tmax1	0.038
bio15	0.108	tmin12	0.054	tmean11	0.046	bio16	0.032
bio16	0.106	bio1	0.053	bio4	0.040	prec8	0.032
bio14	0.106	tmax3	0.052	tmin1	0.039	bio14	0.031
bio12	0.104	tmean11	0.049	tmean6	0.039	tmin8	0.028
prec9	0.100	tmean4	0.049	prec3	0.038	tmean2	0.028
prec8	0.098	bio11	0.041	tmax9	0.037	tmin10	0.028
prec10	0.098	tmean12	0.039	bio6	0.032	tmax5	0.027
prec12	0.096	bio9	0.037	ts_clay	0.031	tmean3	0.025
ts_sand	0.089	tmin4	0.035	tmax7	0.031	bio10	0.025
prec1	0.078	tmean2	0.031	bio14	0.024	tmax12	0.022

bio3	0.068	x_mod	0.030	tmax8	0.023	tmax11	0.022
ts_clay	0.064	ts_loam	0.030	tmean12	0.022	prec9	0.019
x_mod	0.055	tmax1	0.029	bio11	0.021	tmax3	0.018
ts_loam	0.055	Altitude	0.023	tmin2	0.014	tmax4	0.016
bio4	0.043	tmax12	0.020	tmean1	0.013	bio12	0.013
prec4	0.034	tmax2	0.008	tmax6	0.010	bio15	0.011
bio7	0.026	bio15	0.008	prec6	0.009	bio5	0.009
prec11	0.017	prec11	0.006	bio19	0.005	bio1	0.006
bio2	0.014	tmean3	0.006	tmax11	0.004	bio13	0.005
bio18	0.005	tmin5	0.003	bio1	0.002	tmin7	0.003
prec5	0.003	tmin11	0.001	Altitude	0.002	tmean6	0.003

**Table S11** Variable loadings/rotations for each of 4 PCs that were used in BAYENV for 10 *mexicana* populations

<b>PC1</b>		<b>PC2</b>		<b>PC3</b>		<b>PC4</b>	
<b>Var</b>	<b>Rot</b>	<b>Var</b>	<b>Rot</b>	<b>Var</b>	<b>Rot</b>	<b>Var</b>	<b>Rot</b>
bio1	0.152	bio4	0.254	bio13	0.308	ts_sand	0.456
tmean4	0.150	prec12	0.235	prec7	0.308	v_mod	0.338
tmean10	0.150	bio7	0.230	bio16	0.303	bio3	0.300
tmean5	0.150	bio19	0.228	prec8	0.295	ts_clay	0.269
tmean11	0.150	prec2	0.226	bio12	0.270	bio2	0.241
tmax11	0.149	prec6	0.219	x_mod	0.246	bio18	0.232
tmin5	0.149	prec1	0.215	prec9	0.238	sq4	0.181
tmax4	0.149	bio3	0.206	prec10	0.228	ts_loam	0.170
tmin10	0.148	bio17	0.191	prec11	0.227	prec2	0.163
tmin4	0.147	prec5	0.187	prec4	0.227	prec9	0.153
tmax5	0.146	prec3	0.183	bio2	0.184	tmax7	0.148
tmax12	0.146	bio14	0.179	sq4	0.179	prec12	0.147
Altitude	0.144	bio18	0.177	bio15	0.164	sq7	0.142
tmean12	0.144	sq7	0.175	ts_sand	0.152	prec3	0.138
tmax10	0.144	prec9	0.135	prec5	0.142	bio19	0.129
bio10	0.144	prec11	0.135	prec6	0.125	bio12	0.120
bio5	0.143	tmin7	0.129	prec1	0.121	tmax8	0.120
tmin6	0.143	tmax6	0.128	bio9	0.103	prec10	0.112
tmin11	0.142	prec10	0.125	bio19	0.095	tmin6	0.108
tmean9	0.142	tmin3	0.121	ts_loam	0.091	x_mod	0.107
bio11	0.141	tmean7	0.119	tmin1	0.084	tmax9	0.097
bio8	0.141	tmin8	0.115	bio6	0.080	tmax12	0.095
bio9	0.141	bio2	0.107	prec2	0.075	tmax10	0.094
tmean2	0.141	tmin1	0.106	prec12	0.074	tmin9	0.093
tmax2	0.140	bio6	0.105	sq7	0.071	bio14	0.088
tmax1	0.140	tmax7	0.104	tmin12	0.070	tmax11	0.076
tmax3	0.140	tmean8	0.104	prec3	0.067	prec5	0.073
tmin9	0.139	tmean3	0.103	tmin11	0.066	tmin8	0.071
tmean6	0.139	tmean6	0.102	bio7	0.065	tmax1	0.071
tmean8	0.139	tmin2	0.102	bio3	0.064	tmax6	0.069



tmax9	0.139	tmean1	0.099	Altitude	0.056	tmin10	0.066
tmean1	0.139	bio8	0.095	tmin10	0.055	tmean12	0.064
tmean3	0.138	tmean2	0.095	ts_clay	0.055	tmin5	0.059
tmin12	0.138	bio15	0.093	tmax2	0.051	tmin7	0.059
tmax8	0.137	tmax9	0.092	tmin7	0.050	tmean7	0.058
tmin2	0.135	tmean9	0.092	tmin6	0.046	tmean1	0.058
tmean7	0.133	bio11	0.090	bio18	0.045	bio15	0.054
tmin8	0.133	tmax8	0.089	tmax8	0.044	bio11	0.053
tmax7	0.133	tmax1	0.087	tmin2	0.043	bio16	0.047
tmin3	0.132	tmin9	0.086	tmax12	0.040	Altitude	0.047
bio6	0.131	tmax2	0.083	tmax3	0.039	prec8	0.047
tmin1	0.131	tmin12	0.080	tmin5	0.038	tmax2	0.045
tmax6	0.130	tmax3	0.079	tmax11	0.034	bio6	0.042
tmin7	0.127	bio10	0.078	tmin8	0.033	bio7	0.041
ts_loam	0.112	prec4	0.077	v_mod	0.032	prec11	0.040
ts_clay	0.111	bio5	0.075	tmax10	0.032	tmean11	0.040
bio15	0.106	ts_clay	0.074	tmin9	0.031	tmin1	0.040
v_mod	0.101	tmean12	0.069	tmean1	0.030	tmean5	0.038
prec4	0.094	x_mod	0.069	tmean5	0.030	tmean2	0.038
bio14	0.091	tmax10	0.063	tmax9	0.029	bio17	0.036
prec3	0.090	tmin6	0.062	tmax1	0.027	tmean8	0.033
bio17	0.089	tmin11	0.056	bio5	0.027	tmin12	0.031
sq7	0.077	tmax5	0.052	tmean6	0.026	bio10	0.029
bio12	0.065	tmax12	0.052	bio10	0.026	bio8	0.029
prec11	0.064	Altitude	0.049	tmax5	0.025	bio4	0.028
prec5	0.062	tmin4	0.048	tmax7	0.022	tmin2	0.027
sq4	0.058	v_mod	0.048	tmean12	0.018	bio1	0.026
prec1	0.055	ts_loam	0.047	tmean11	0.017	tmax5	0.024
prec8	0.052	bio12	0.046	bio11	0.014	bio13	0.021
prec10	0.051	bio13	0.040	tmean3	0.012	prec7	0.021
bio18	0.048	prec7	0.040	bio14	0.012	prec4	0.017
prec9	0.043	bio9	0.040	tmin3	0.012	tmax3	0.017
prec2	0.042	tmean10	0.035	tmean10	0.011	tmean9	0.017

bio19	0.035	bio16	0.030	tmean7	0.011	tmin4	0.016
bio2	0.032	ts_sand	0.028	tmax6	0.010	tmean10	0.016
bio16	0.032	tmean4	0.028	bio8	0.010	prec6	0.016
x_mod	0.029	sq4	0.025	bio1	0.010	bio9	0.012
prec12	0.025	tmean11	0.023	bio17	0.008	tmean3	0.010
bio7	0.022	tmean5	0.021	tmax4	0.008	tmax4	0.010
bio13	0.019	tmax11	0.013	tmean8	0.007	bio5	0.008
prec7	0.019	tmin5	0.013	tmin4	0.007	tmean6	0.008
prec6	0.017	tmax4	0.009	bio4	0.004	tmin11	0.007
bio3	0.003	tmin10	0.004	tmean9	0.004	tmean4	0.006
bio4	0.003	bio1	0.002	tmean2	0.003	prec1	0.002
ts_sand	0.000	prec8	0.001	tmean4	0.003	tmin3	0.001

**Text S1** List of 278 maize inbred lines used in the association analysis

33.16, 38.11, 4226, 4722, A188, A214N, A239, A272, A441.5, A554, A556, A6, A619, A632, A634, A635, A641, A654, A659, A661, A679, A680, A682, AB28A, B10, B103, B104, B105, B109, B115, B14A, B164, B2, B37, B46, B52, B57, B64, B68, B73, B73HTRHM, B75, B76, B77, B79, B84, B97, C103, C123, C49A, CH701.30, CH9, CI.7, CI187.2, CI21E, CI28A, CI31A, CI3A, CI64, CI66, CI90C, CI91B, CM105, CM174, CM37, CM7, CML10, CML103, CML108, CML11, CML14, CML154Q, CML157Q, CML158Q, CML218, CML220, CML228, CML238, CML247, CML254, CML258, CML261, CML264, CML277, CML281, CML287, CML311, CML314, CML321, CML322, CML323, CML328, CML331, CML332, CML333, CML341, CML38, CML45, CML5, CML52, CML61, CML69, CML77, CML91, CML92, CMV3, CO106, CO125, CO255, D940Y, DE.2, DE.3, DE1, DE811, E2558W, EP1, F2834T, F44, F6, F7, GA209, GT112, H105W, H49, H84, H91, H95, H99, HI27, HP301, HY, I137TN, I205, I29, IA2132, IA5125, IDS28, IDS69, IDS91, IL101, IL14H, IL677A, K148, K4, K55, K64, KI11, KI14, KI2021, KI21, KI3, KI43, KI44, KY21, KY226, KY228, L317, L578, M14, M162W, M37W, MEF156.55.2, MO17, MO18W, MO1W, MO24W, MO44, MO45, MO46, MO47, MOG, MP339, MS1334, MS153, MS71, MT42, N192, N28HT, N6, N7A, NC222, NC230, NC232, NC236, NC238, NC250, NC258, NC260, NC262, NC264, NC290A, NC294, NC296, NC296A, NC298, NC300, NC302, NC304, NC306, NC310, NC314, NC318, NC320, NC324, NC326, NC328, NC33, NC336, NC338, NC340, NC342, NC344, NC346, NC348, NC350, NC352, NC354, NC356, NC358, NC360, NC362, NC364, NC366, NC368, ND246, OH40B, OH43, OH43E, OH603, OH7B, OS420, P39, PA762, PA875, PA880, PA91, R109B, R168, R177, R229, R4, SA24, SC213R, SC357, SC55, SD40, SD44, SG1533, SG18, T232, T234, T8, TX303, TX601, TZI10, TZI11, TZI16, TZI18, TZI25, TZI9, U267Y, VA102, VA14, VA17, VA22, VA26, VA35, VA59, VA85, VA99, VAW6, W117HT, W153R, W182B, W22, WD, WF9, YU796.NS